

**SUB-APPENDIX G-2**  
**IH2VOF MODELING REPORT**

This page intentionally left blank.

**SOUTHERN PALM BEACH ISLAND COMPREHENSIVE  
SHORELINE STABILIZATION PROJECT  
IH2VOF MODELING REPORT**

**TABLE OF CONTENTS**

**1.0 INTRODUCTION** ..... Error! Bookmark not defined.

**2.0 IH2VOF** ..... Error! Bookmark not defined.

**2.1. Governing Equations** ..... Error! Bookmark not defined.

**2.2. Wave Maker** ..... Error! Bookmark not defined.

**2.3. Volume of Fluid Method** ..... Error! Bookmark not defined.

**2.4. Overtopping Damage Criteria** ..... Error! Bookmark not defined.

**2.5. Input Data and Simulated Scenarios** ..... Error! Bookmark not defined.

**3.0 RESULTS** ..... Error! Bookmark not defined.

**3.1. T-131** ..... **16**

**3.2. R-137** ..... Error! Bookmark not defined.

**4.0 WAVE FORCES ON SEAWALL** ..... Error! Bookmark not defined.

**5.0 SUMMARY** ..... Error! Bookmark not defined.

**6.0 CONCLUSIONS** ..... Error! Bookmark not defined.

**7.0 LITERATURE CITED** ..... Error! Bookmark not defined.

## LIST OF FIGURES

### Figure No.

2-1	Critical overtopping discharge according to USACE (2006). .....	6
2-2	IH2VOF input profiles taken from SBEACH at event peak for existing conditions and for alternative 2/6. T-131 (top) and R-137 (bottom). .....	7
2-3	Wave profiles at T-131 and R-137 for return period waves of 15 (green), 25 (blue), 50 (red) and 100 (cyan) years. ....	8
2-4	15 years return period waves – $\eta$ timeseries, wave height and period histograms, JONSWAP spectrum, $H_s \times T_p$ and U and V velocity fields.....	10
2-5	25 years return period waves – $\eta$ timeseries, wave height and period histograms, JONSWAP spectrum, $H_s \times T_p$ and U and V velocity fields.....	11
2-6	50 years return period waves – $\eta$ timeseries, wave height and period histograms, JONSWAP spectrum, $H_s \times T_p$ and U and V velocity fields.....	12
2-7	100 years return period waves at T-131– $\eta$ timeseries, wave height and period histograms, JONSWAP spectrum, $H_s \times T_p$ and U and V velocity fields. ....	13
2-8	100 years return period waves at R-137– $\eta$ timeseries, wave height and period histograms, JONSWAP spectrum, $H_s \times T_p$ and U and V velocity fields. ....	14
2-9	IH2VOF numerical grid and a zoom-in view at swash zone: beach profile (yellow) and water level (cyan). ....	15
3-1	T-131 - 15 year return period wave at 906.5 s of simulation for existing (top) and Alternative 2/6 (bottom). ....	18
3-2	T-131 - 25 year return period wave at 465 s of simulation for existing (top) and Alternative 2/6 (bottom). ....	19
3-3	T-131 - 50 year return period wave at 644 s of simulation for existing (top) and Alternative 2/6 (bottom). ....	20
3-4	T-131 - 100 year return period wave at 484.5 s of simulation for existing (top) and Alternative 2/6 (bottom). ....	21
3-5	T-131 – 15 year return period wave $\eta$ at probes 1 to 7.....	23
3-6	T-131 – 25 year return period wave $\eta$ at probes 1 to 7.....	24
3-7	T-131 – 50 year return period wave $\eta$ at probes 1 to 7.....	25

3-8	T-131 – 100 year return period wave $\eta$ at probes 1 to 7.....	26
3-9	Overtopping results – T-131 - 15 year return period for existing conditions (black) and with alternative (green). .....	29
3-10	Overtopping results – T-131 - 25 year return period for existing conditions (black) and with alternative (green). .....	30
3-11	Overtopping results – T-131 - 50 year return period for existing conditions (black) and with alternative (green). .....	31
3-12	Overtopping results – T-131 - 100 year return period for existing conditions (black) and with alternative (green). .....	32
3-13	R-137 - 15 year return period wave at 499.4 s of simulation for existing (top), Alternative 2 (centre) and Alternative 6 (bottom). .....	34
3-14	R-137 - 25 year return period wave at 465 s of simulation for existing (top), Alternative 2 (centre) and Alternative 6 (bottom). .....	35
3-15	R-137 - 50 year return period wave at 440 s of simulation for existing (top), Alternative 2 (centre) and Alternative 6 (bottom). .....	36
3-16	R-137 - 100 year return period wave at 458.5 s of simulation for existing (top), Alternative 2 (centre) and Alternative 6 (bottom). .....	37
3-17	R-137 – 15 year return period wave $\eta$ at probes 1 to 7. ....	40
3-18	R-137 – 25 year return period wave $\eta$ at probes 1 to 7. ....	41
3-19	R-137 – 50 year return period wave $\eta$ at probes 1 to 7. ....	42
3-20	R-137 – 100 year return period wave $\eta$ at probes 1 to 7. ....	43
3-21	Overtopping results – R-137 - 15 year return period for existing conditions (black), Alternative 2 (green), Alternative 6 (red). .....	45
3-22	Overtopping results – R-137 - 25 year return period for existing conditions (black), Alternative 2 (green), Alternative 6 (red). .....	46
3-23	Overtopping results – R-137 - 50 year return period for existing conditions (black), Alternative 2 (green), Alternative 6 (red). .....	47
3-24	Overtopping results – R-137 - 100 year return period for existing conditions (black), Alternative 2 (green), Alternative 6 (red). .....	48

4-1 Dynamic load at seawall: top to bottom: Existing condition RP15, Existing condition RP25, Existing condition RP50, Existing condition RP100..... 51

**LIST OF TABLES**

**Table No.**

2-1 Offshore significant wave height at IH2VOF boundary..... 9  
2-2 Offshore wave and water level conditions simulated on IH2VOF..... 16  
3-1 Mean overtopping discharge summary for all cases..... 49

## 1.0 INTRODUCTION

Under direction of the U.S. Army Corps of Engineers (USACE), CB&I Coastal Planning & Engineering, Inc. (CB&I) assisted in the development of the Southern Palm Beach Island Comprehensive Shoreline Stabilization Project Environmental Impact Statement (EIS). The initial tasks associated with the effort included public scoping and agency coordination to determine what data was necessary to develop the EIS. After review of the data and previous work, the USACE determined that numerical modeling of seawall overtopping and wave forces was required to obtain necessary data that is not currently available.

The upland property along Southern Palm Beach Island is at risk of flooding if seawalls fail or are overtopped by waves. It was necessary to assess the potential for seawall overtopping as well as the wave generated forces on it. To do that, the IH2VOF model was applied. The model solves the Reynolds-Averaged Navier-Stokes equation using a Volume-of-Fluid (VOF) Approach. The storm profiles generated during the SBEACH analysis of alternatives (CB&I, 2014) were used to analyze the potential wave overtopping and to provide visual and numerical results. The model was also used to evaluate wave forces on seawalls.

Two locations were simulated in IH2VOF, one without a seawall (T-131) and one with a seawall (R-137). At each location, the existing condition (SBEACH storm profile) and two alternatives were simulated and compared. The alternatives that were considered in the analysis included:

- Alternative 2 – Applicants' Preferred Project (Proposed Action): Beach and Dune Fill with Shoreline Protection Structures
- Alternative 6 – The Town of Palm Beach Increased Sand Volume and County Increased Sand Volume without Shoreline Protection Structures

The remainder of the alternatives (Alternatives 3, 4, 5, 7a and 7b) were not included in the analysis. Alternative 3 included the same fill volume as Alternative 2, but without shore

protection structures. Alternatives 4 and 5 were combinations of Alternatives 2 and 6. Alternative 1 was considered the No Action Alternative (Status Quo) and was represented by the comparisons with the existing conditions. Alternatives 7a and 7b were not considered when the model was originally run and are therefore not included in the analysis.

## 2.0 IH2VOF

IH2VOF is a two-dimensional (vertical) wave model developed by IH Cantabria. The model can be applied to a wide range of cases including coastal, ocean, offshore and hydraulic engineering.

### 2.1. Governing Equations

IH2VOF solves the two-dimensional wave flow for hybrid domain based on coupled Navier-Stokes-type equations. The hybrid domain contains two parts: the clear fluid region and the porous media region. At the clear fluid region, the coupled Reynolds Averaged Navier–Stokes (RANS) equations system is implemented. The Volume-Averaged Reynolds Averaged Navier–Stokes (VARANS) equations are used inside the porous media regions. IH2VOF simulates both mean flow and turbulence with the  $\kappa$ - $\varepsilon$  equations for the turbulent kinetic energy  $\kappa$ , and the dissipation rate  $\varepsilon$ . It permits the modeling of wave flow against any kind of coastal structure (e.g. rubble mound, vertical or mixed breakwaters). The free surface movement is tracked by the volume of fluid (VOF) method.

The RANS equations (clear fluid region) are redefined as follows:

$$\frac{\partial \bar{u}_i}{\partial x_i} = 0$$

$$\frac{\partial \bar{u}_i}{\partial t} + \bar{u}_j \frac{\partial \bar{u}_i}{\partial x_j} = -\frac{1}{\rho} \frac{\partial \bar{p}}{\partial x_i} + g_i + \frac{1}{\rho} \frac{\partial \bar{\tau}_{ij}}{\partial x_j} - \frac{\partial \overline{(u_i' u_j')}}{\partial x_j}$$

where  $\rho$  is the density of the fluid,  $g_i$  is the  $i_{th}$  component of the gravitational acceleration and  $\tau_{ij}$  is the mean viscous stress tensor.

The flow inside the porous media is modeled by solving the VARANS equations, first presented by Hsu et al. (2002). These equations are derived by integrating the RANS equations over a control volume, and their final form is presented below:

$$\frac{\partial \langle \bar{u}_i \rangle}{\partial x_i} = 0$$

$$\frac{\partial \langle \bar{u}_i \rangle}{\partial t} + \frac{\langle \bar{u}_j \rangle}{1 + C_A} \frac{\partial \langle \bar{u}_i \rangle}{\partial x_j} = \frac{1}{\rho(1 + C_A)} \left[ -\frac{\partial \langle \bar{P} \rangle}{\partial x_i} - \frac{\partial \rho \langle \bar{u}_i \bar{u}_j' \rangle}{\partial x_j} + \frac{\partial \langle \bar{\tau}_{ij} \rangle}{\partial x_j} + \rho g_i \right] - \frac{1}{1 + C_A} \left[ \alpha v \frac{(1-n)^2}{n^2 D_{50}^2} \langle \bar{u}_i \rangle + \frac{\beta(1-n)}{n D_{50}^2} \sqrt{\langle \bar{u}_1 \rangle^2 \langle \bar{u}_2 \rangle^2} \langle \bar{u}_i \rangle \right]$$

In the free fluid region, i.e, with  $n = 1$  and  $C_A = 0$ , the VARANS equations is synonymous with the original RANS equations.

## 2.2. Wave Maker

Wave generation is a key factor for numerical models devoted to coastal engineering, as the generated waves have to resemble observation in the field and laboratory. Several wave generation methods are implemented in IH2VOF in order to compare their abilities to reproduce realistic waves. The mechanisms of wave generation include internal wave maker, static wave paddle (Dirichlet boundary condition) and dynamic wave paddle (virtual force method). In this study, the static wave paddle was used. The theory of static wave paddle gives analytical expressions for free surface and the velocity distribution throughout the water column. It is the simplest and most commonly used wave maker in wave models. The static wave paddle can also be used to replicate the behavior of any laboratory wave paddle such as a piston-type wave generator.

## 2.3. Volume of Fluid Method

In the IH2VOF model, the free surface is tracked using the Volume of Fluid (VOF) method presented by Hirt and Nichols (1981). Instead of pursuing the exact location of the free surface, this method identifies the free surface by tracking the density change in each

grid cell. The model identifies three cell types: empty (E), surface (S) and interior (I) cells depending on the value of the VOF function  $F$  defined as follows:

$$F = \frac{\rho}{\rho_f}$$

Where

$$\rho = \frac{\rho_f V_f}{V_f + V_a}$$

being  $\rho$  the fluid density,  $V$  the volume of fluid in the cell, and  $V_a$  the volume of air in the cell.

Empty cell is defined as  $F = 0$ , which contains only air. Interior cell is defined as  $F = 1$ , which contains pure fluid. Surface cell is defined as  $1 > F > 0$ , which contains both fluid and air. The introduction of the VOF function in the equation of mass conservation yields the transport equation for  $F(x, y, t)$ :

$$\begin{aligned} \rho(x, y, t) &= F(x, y, t)\rho_f \\ \frac{\partial F}{\partial t} + \frac{\partial}{\partial x}(\bar{u}F) + \frac{\partial}{\partial y}(\bar{v}F) &= 0 \end{aligned}$$

## 2.4. Overtopping Damage Criteria

According to Peng and Zou (2011), overtopping is defined as the volume of water that passes over the crest of a structure per one unit of length per one unit of time. The mean discharge is expressed in  $\text{m}^3/\text{m}/\text{s}$ . EurOtop (2007) describes the overtopping discharge over a structure crest as a random process over time and volume due to wave nonlinearity. Larger waves will overtop greater quantities of water in a short time period (less than a wave period), smaller waves may not produce any overtopping.

Several important factors contributing to the overtopping process due to waves have been identified including wave height and period, the structure (or dune) elevation, structure (or

beach) slope, water thickness and current velocity at the top of the structure (Schüttrumpf and Oumeraci, 2005; Lykke Andersen et. al., 2006; Van der Meer et. al., 2009). EutOtop (2007) classified the mean overtopping discharge ( $q$ ) according to the impact factor:

$q < 0.1$  liters/s/m: Insignificant with respect to strength of crest and rear of structure;

$q = 1$  liters/s/m: On crest and inner slopes grass and/or clay may start to erode;

$q = 10$  liters/s/m: Significant overtopping for dikes and embankments. Some overtopping for rubble mound breakwaters;

$q = 100$  liters/s/m: Crest and inner slopes of dikes have to be protected by asphalt or concrete; for rubble mound breakwaters transmitted waves may be generated.

The Coastal Engineering Manual (USACE, 2006) compiled information from a series of studies in a table that presents the critical values of mean overtopping discharge (Figure 2-1). The values presented should be considered as guidelines because for a given amount of instantaneous overtopping, the damage caused by the overtopped water largely depends on the geometry of structure (or beach profile) and the distance from the structure. Maximum intensity may be locally two orders of magnitude greater than the mean overtopping discharge. The acceptable condition is a matter that varies depending on the location and the objective of each project.

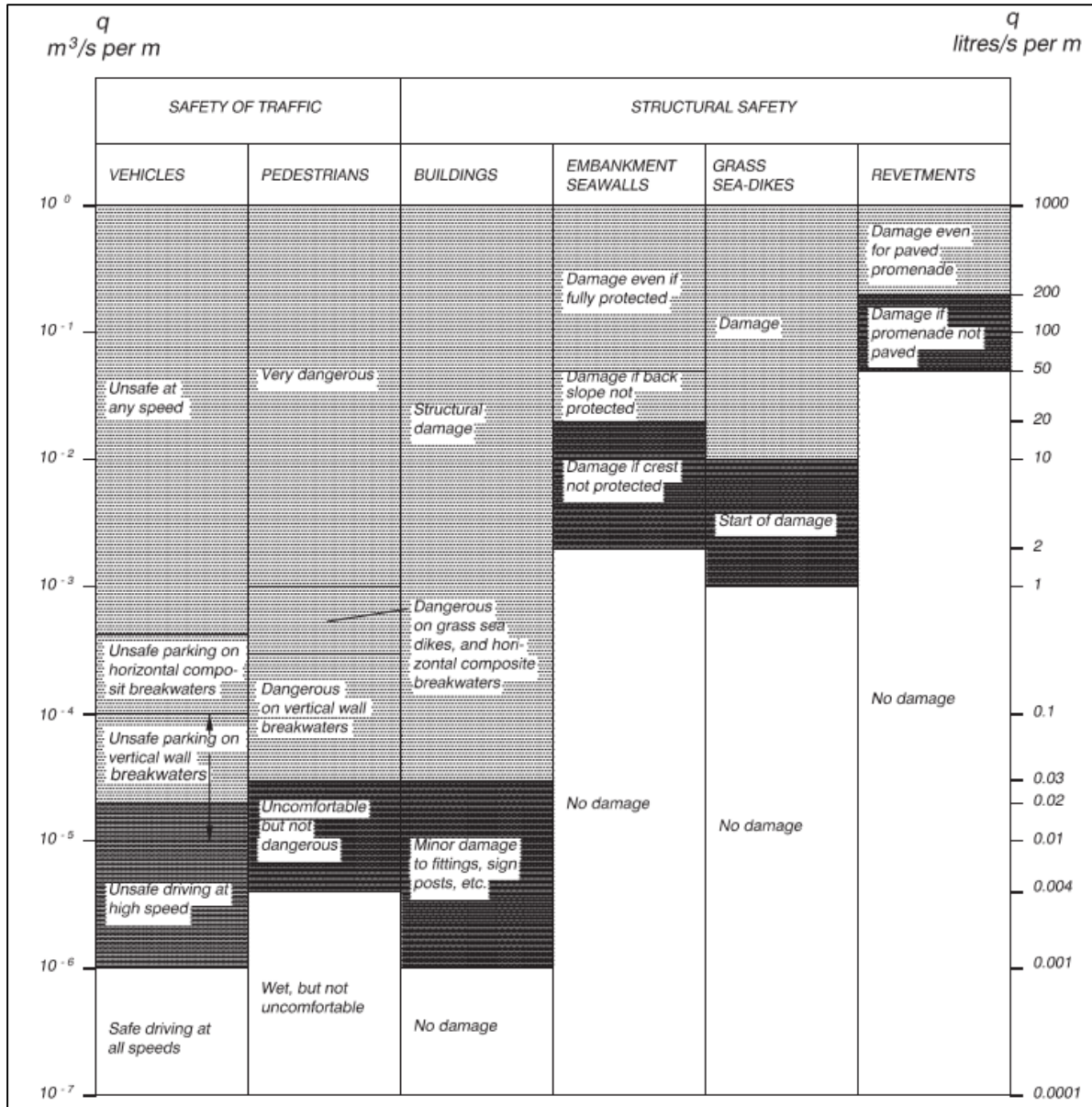
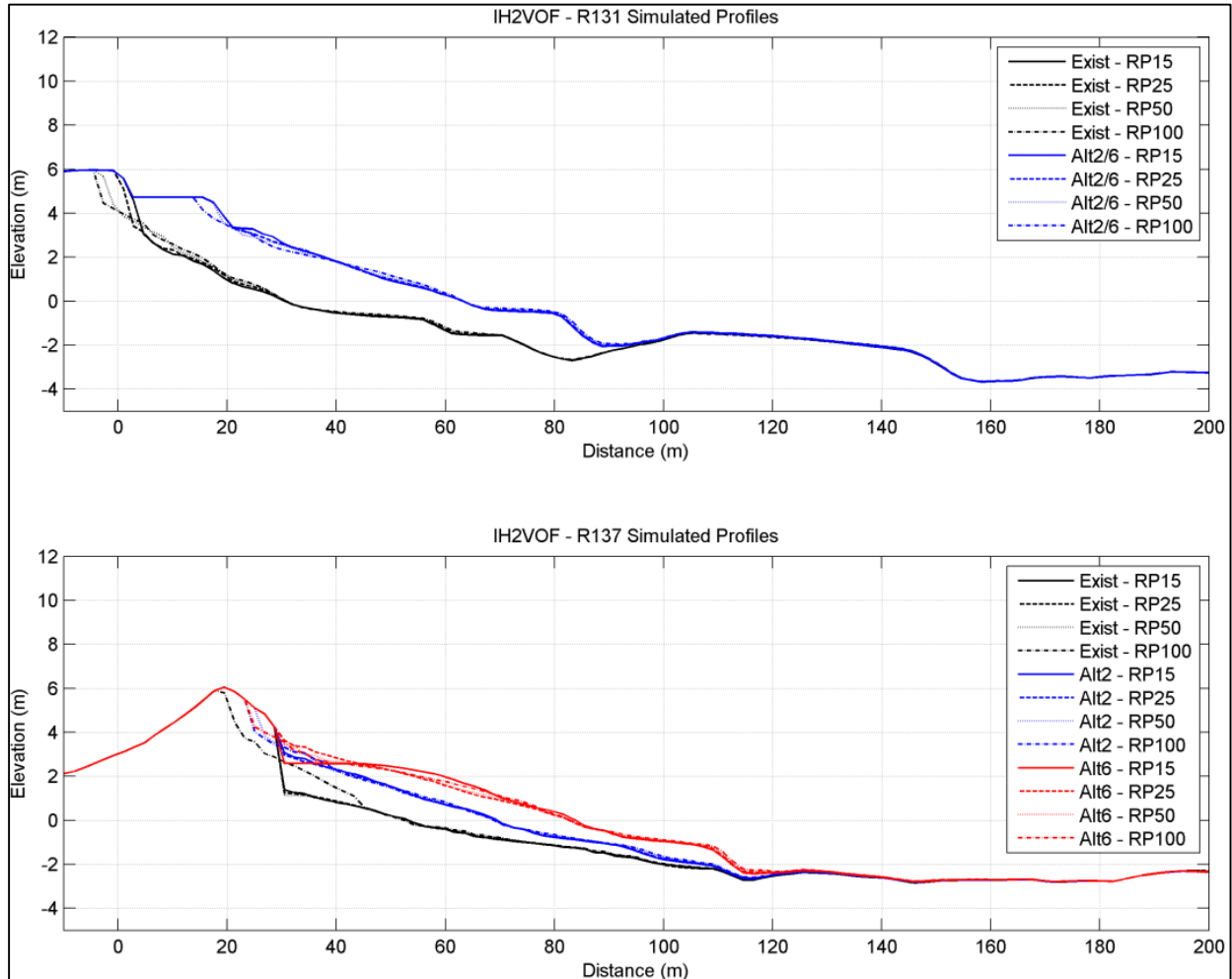


Figure 2-1. Critical overtopping discharge according to USACE (2006).

### 2.5. Input Data and Simulated Scenarios

Input data for the IH2VOF model consists of beach profile, water level, and wave conditions. Two locations were simulated: one without a seawall (T-131) and one with a seawall (R-137). Alternative 2 represented the smallest beach fill quantity, while Alternative 6 represented the largest volume. The beach fills’ response to storm events were first modeled in SBEACH. The storm profiles were taken from SBEACH simulation

(CB&I, 2014) at the event peak for each alternative. At T-131, both alternatives (2 and 6) are identical. Figure 2-2 shows the input profiles at T-131 and R-137 with elevation in meters referenced to mean sea level.



**Figure 2-2. IH2VOF input profiles taken from SBEACH at event peak for existing conditions and for Alternative 2/6. T-131 (top) and R-137 (bottom).**

The water level used in IH2VOF was also taken from the SBEACH simulations (CB&I, 2014) and was defined as a constant elevation above mean sea level. For storm return periods (RP) storms of 15, 25, 50 and 100 years, the water level considered was 1.52, 1.68, 1.92 and 2.13 m, respectively.

Wave conditions were also obtained from the SBEACH simulation (CB&I, 2014The wave parameters presented). At event peak, the wave profile was analyzed and the values were

obtained at a distance coincident to the IH2VOF offshore boundary, which was approximately 500 m seaward of the range monuments (R-monuments). Four extreme wave conditions were simulated (15, 25, 50 and 100 years return period) for each alternative and the existing profile (Figure 2-3).

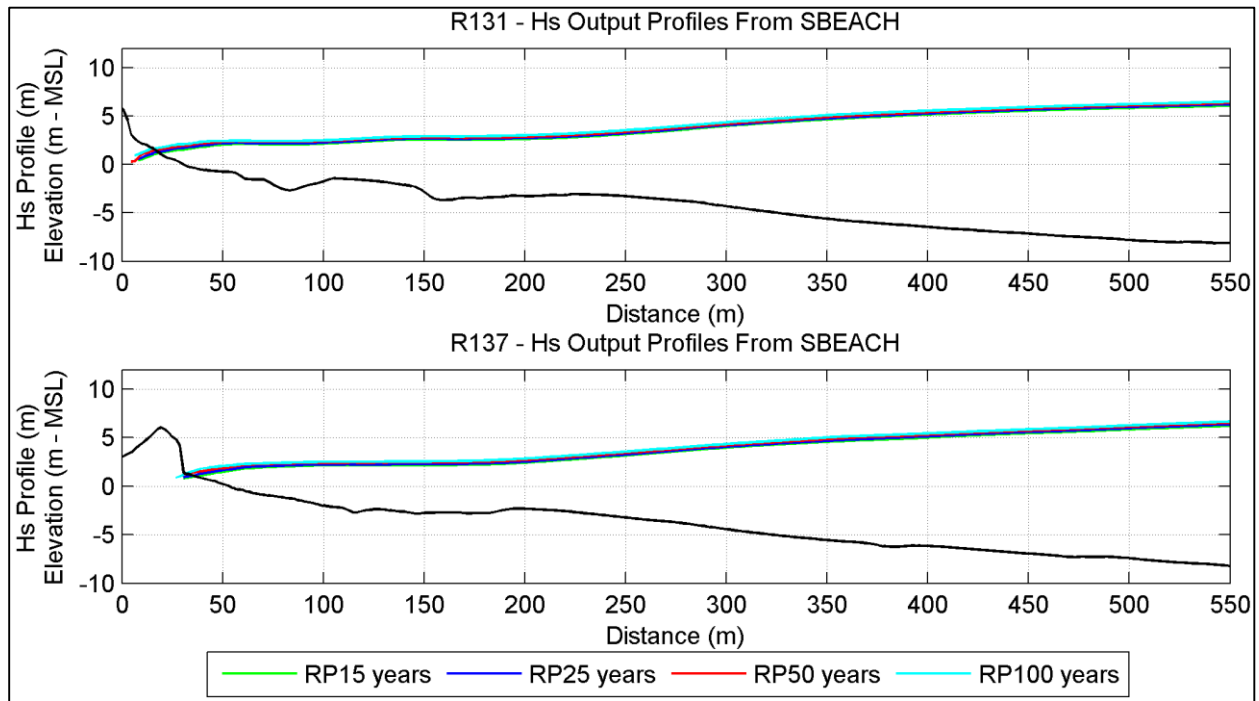


**Figure 2-3 Wave profiles at T-131 and R-137 for return period waves of 15 (green), 25 (blue), 50 (red) and 100 (cyan) years.**

Differences between wave conditions for both profiles as well as between alternatives are presented in Table 2-1.

Regardless of the alternatives or existing conditions, it can be seen that the significant wave heights varied between the two profiles by less than 0.01 m, 0.02 m and 0.04 m for the 15, 25 and 50-year return period waves, respectively. This represented a difference of less than 0.1% between the wave heights for all alternatives, which was considered negligible. For this reason, the same wave condition was imposed at the IH2VOF boundary at T-131 and R-137 profiles for each return period wave (5.86 m for 15-year, 5.99 m for 25-year, and 6.16 m for 50-year) (see Figure 2-4 to Figure 2-6). For the 100-year return period wave, the significant wave height varied between the profiles T-131 (6.33 m) and R-137 (6.55 m) (Figure 2-7 and Figure 2-8). Based on this difference, profiles

T-131 and R-137 were run with different significant wave heights at the IH2VOF boundary.

**Table 2-1. Offshore significant wave height at IH2VOF boundary.**

Return period / Case (year)	T-131 (m)		R-137 (m)		
	Existing	Alternative 2/6	Existing	Alternative 2	Alternative 6
15	5.85	5.85	5.86	5.86	5.86
25	5.97	5.97	5.99	5.99	5.99
50	6.12	6.12	6.16	6.14	6.14
100	6.33	6.33	6.55	6.55	6.55

The wave parameters presented above were used in IH2VOF wave maker, which generated irregular wave timeseries. Based on the wave timeseries, the horizontal (U) and vertical (V) current velocity field were also imposed at model boundary for continuity. The timeseries, histograms, spectrum and Hs x Tp and U and V field plots are presented below for 15-year (Figure 2-4), 25-year (Figure 2-5), 50-year (Figure 2-6), and 100-year return period waves at T-131 (Figure 2-7) and 100-year return period waves at R-137 (Figure 2-8).

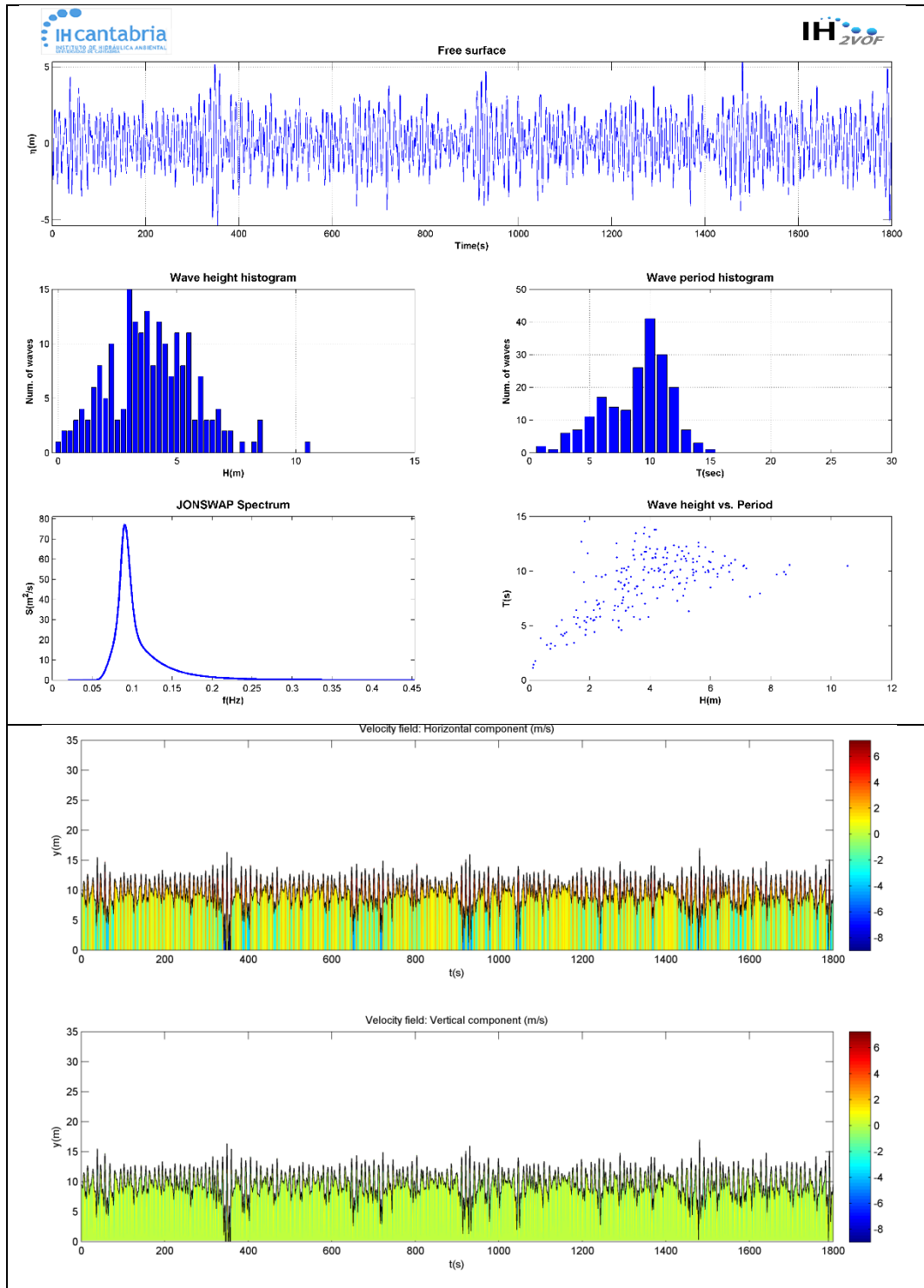
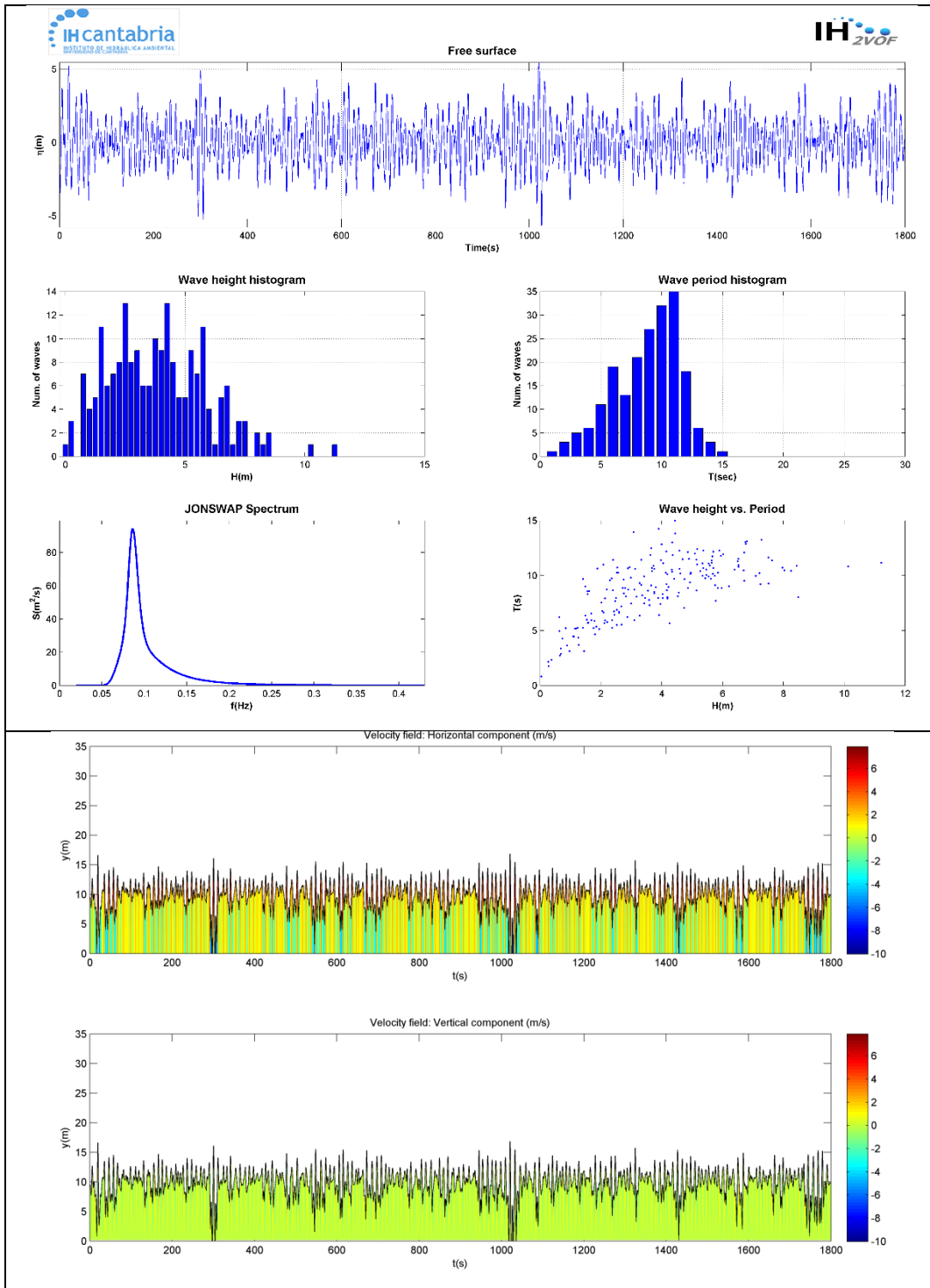
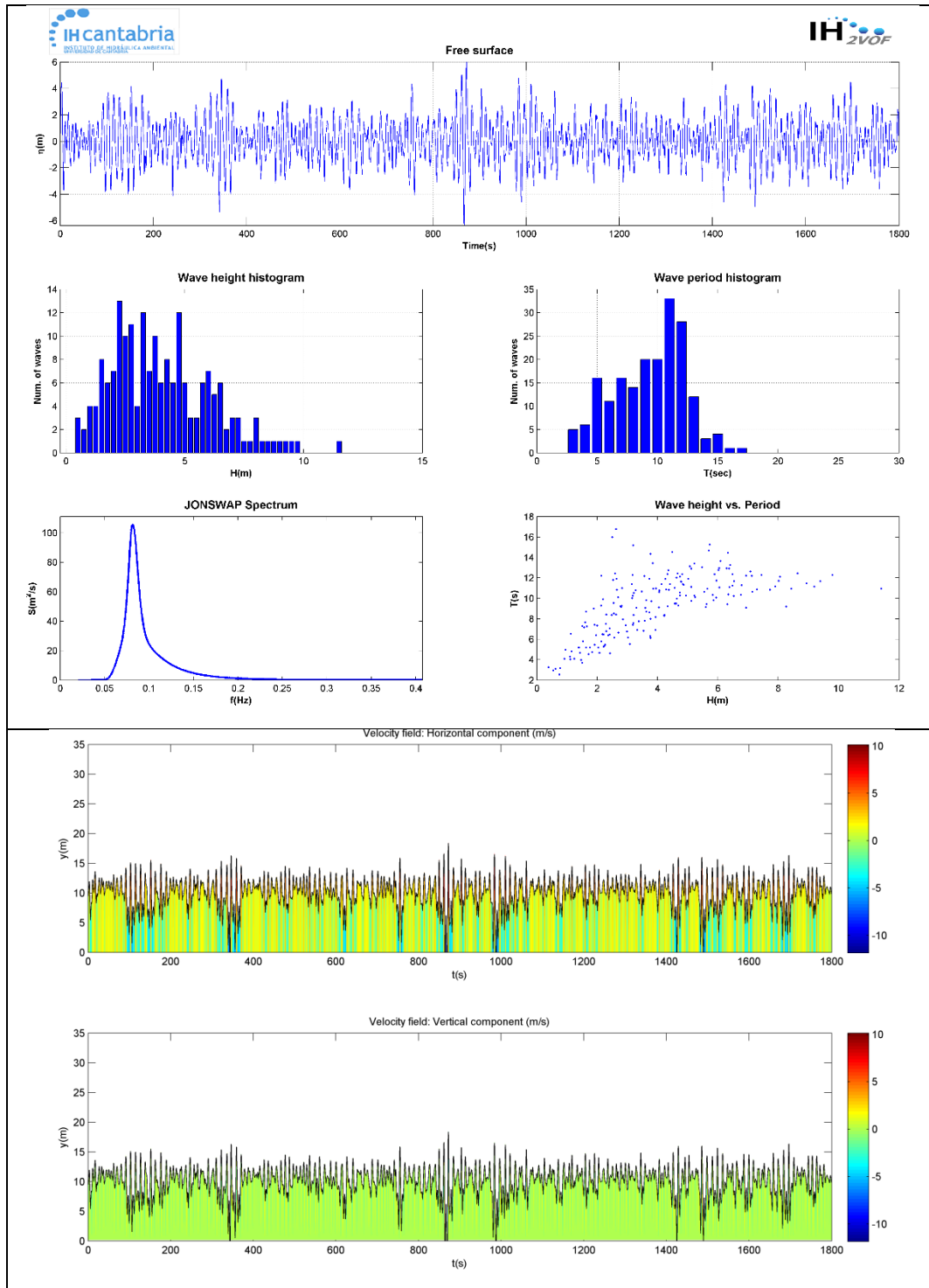


Figure 2-4. 15 year return period waves –  $\eta$  timeseries, wave height and period histograms, JONSWAP spectrum,  $H_s \times T_p$  and U and V velocity fields.



**Figure 2-5. 25 year return period waves –  $\eta$  timeseries, wave height and period histograms, JONSWAP spectrum,  $H_s \times T_p$  and U and V velocity fields.**



**Figure 2-6. 50 year return period waves –  $\eta$  timeseries, wave height and period histograms, JONSWAP spectrum,  $H_s \times T_p$  and U and V velocity fields.**

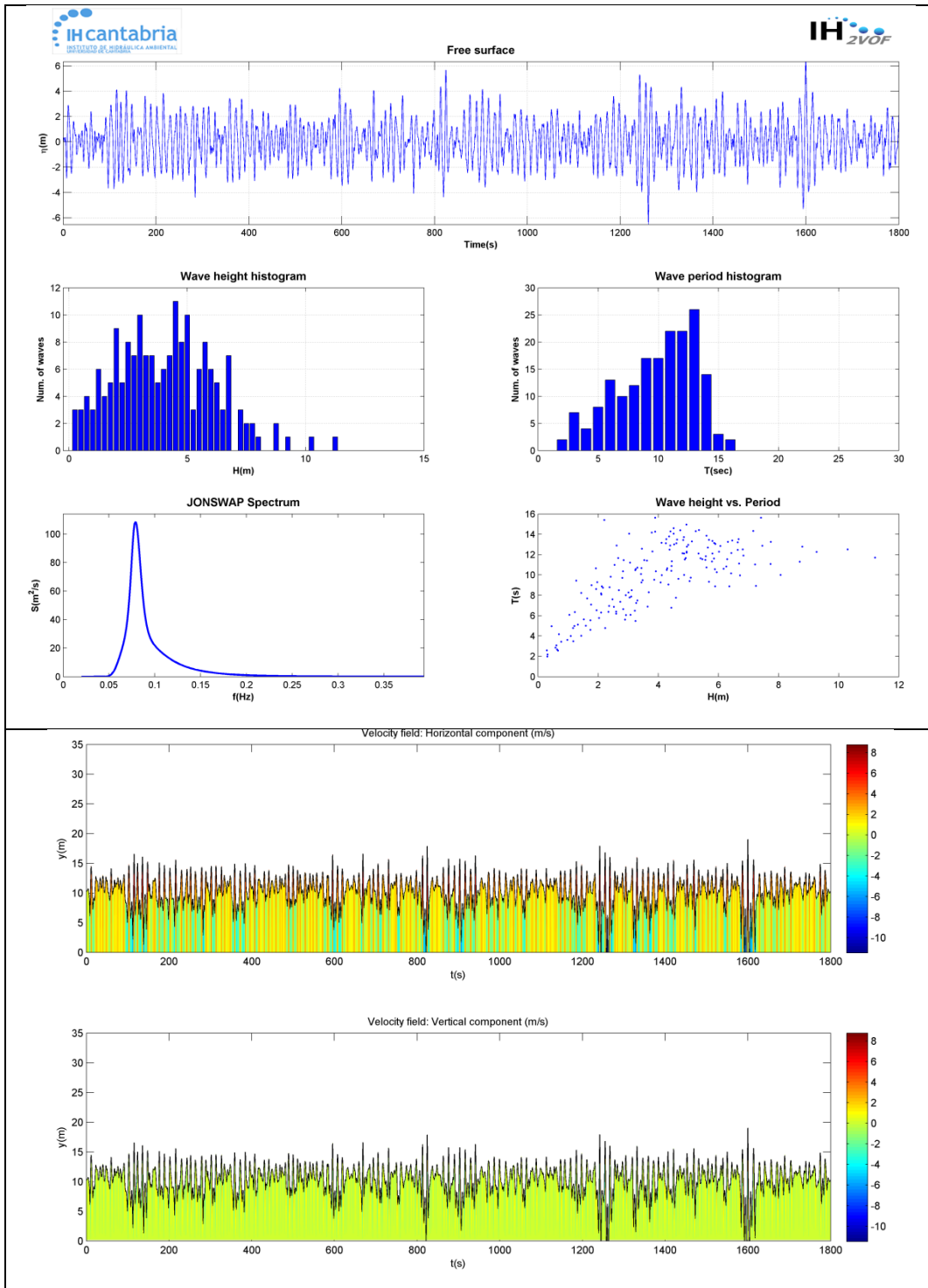


Figure 2-7. 100 year return period waves at T-131 –  $\eta$  timeseries, wave height and period histograms, JONSWAP spectrum,  $H_s \times T_p$  and U and V velocity fields.

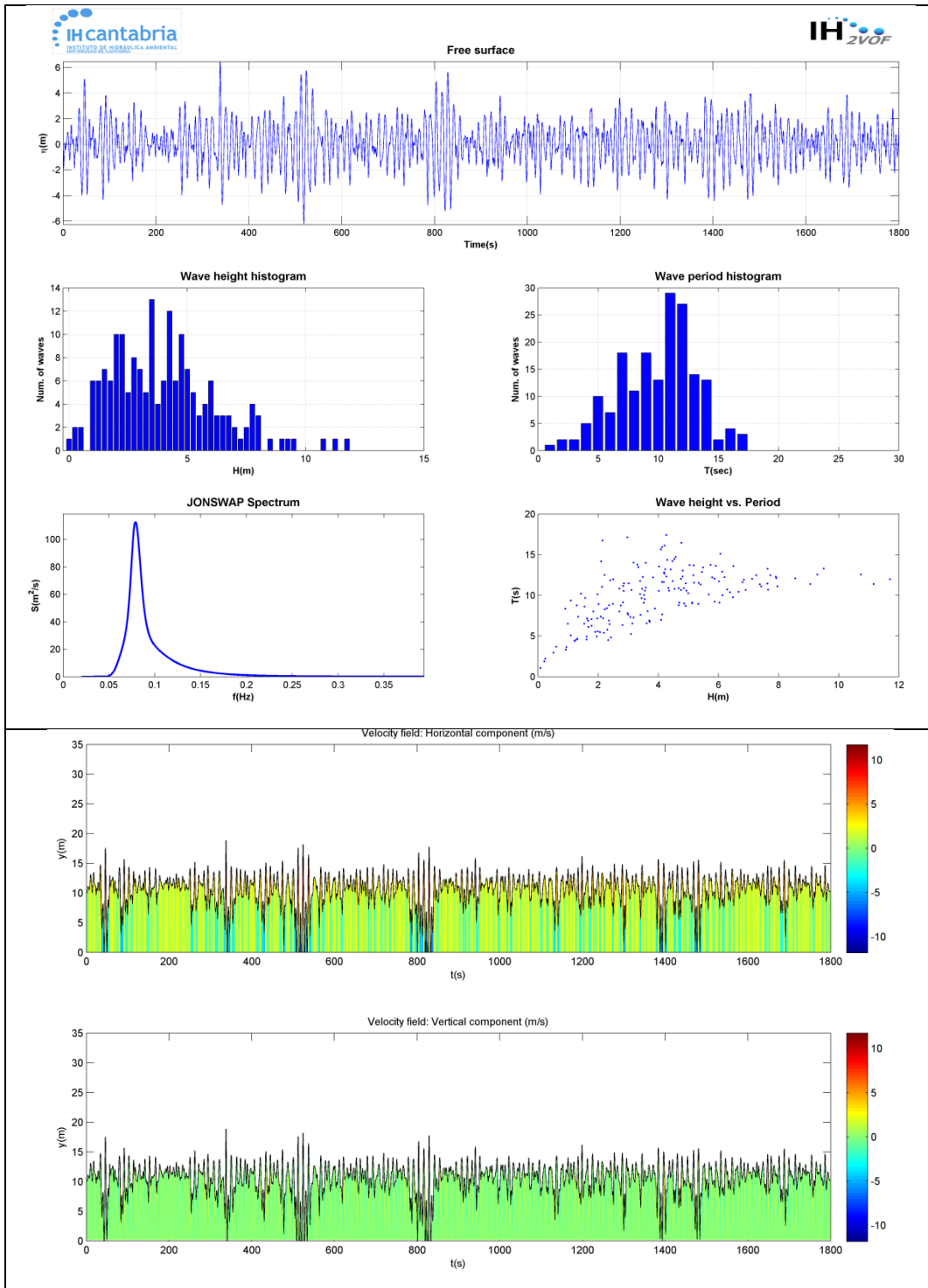
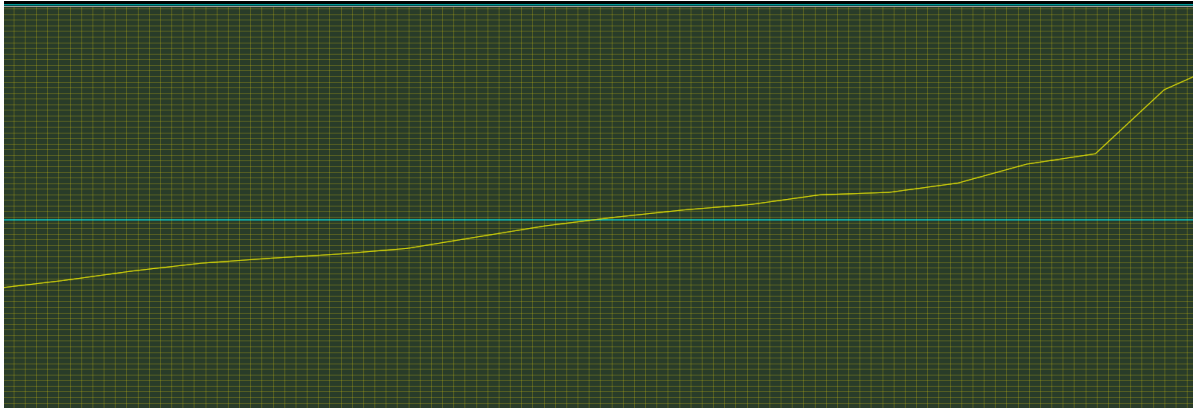


Figure 2-8. 100 year return period waves at R-137–  $\eta$  timeseries, wave height and period histograms, JONSWAP spectrum,  $H_s \times T_p$  and U and V velocity fields.

The regular numerical grid used in IH2VOF consists of a 2DV grid of 501 meter x 35.1 meter (1670 x 234 numerical elements) with horizontal resolution of 0.3 meter and vertical resolution of 0.15 meter (Figure 2-9). The recommended relation of  $D_x < 2.5 D_y$  was maintained to avoid wave false breaking. The grids and outputs from IH2VOF model are oriented with landward being to the right and offshore to the left. For reference, this is opposite of the orientation of the SBEACH profiles shown in Figure 2-2 and Figure 2-3.



**Figure 2-9. IH2VOF numerical grid and a zoom-in view at swash zone: beach profile (yellow) and water level (cyan).**

A total of 20 simulations were conducted at T-131 and R-137. The return period storm conditions of 15, 25, 50 and 100 years were considered for the existing condition and the alternatives. A summary of simulated scenarios are presented in Table 2-2. All the simulations started with a constant water level condition (cold start). Thus, the first 5 minutes were considered as the “spinup” time and were not used in the analysis presented below. Following the “spinup” time, the total analysis time was 25 minutes (1500 seconds). It is important to highlight that the swash zone is a very active zone with nonlinear wave interactions. The wave randomness and nonlinear wave interactions may cause a single overtopping wave to occur higher in a wider beach than existing condition, while the frequency and cumulative overtopping are less. To avoid misinterpretation, a period of 25 minutes was chosen, so the stochastic events are minimized and the mean condition is considered.

**Table 2-2. Offshore wave and water level conditions simulated on IH2VOF.**

Profile	Condition	Return Period (years)	Hs (m)	Tp (s)	Water Level (m)
T-131	Existing	15	5.86	11.0	1.52
	Existing	25	5.99	11.5	1.68
	Existing	50	6.16	12.2	1.92
	Existing	100	6.33	12.8	2.13
T-131	Alternative 2/6	15	5.86	11.0	1.52
	Alternative 2/6	25	5.99	11.5	1.68
	Alternative 2/6	50	6.16	12.2	1.92
	Alternative 2/6	100	6.33	12.8	2.13
R-137	Existing	15	5.86	11.0	1.52
	Existing	25	5.99	11.5	1.68
	Existing	50	6.16	12.2	1.92
	Existing	100	6.55	12.8	2.13
R-137	Alternative 2	15	5.86	11.0	1.52
	Alternative 2	25	5.99	11.5	1.68
	Alternative 2	50	6.16	12.2	1.92
	Alternative 2	100	6.55	12.8	2.13
R-137	Alternative 6	15	5.86	11.0	1.52
	Alternative 6	25	5.99	11.5	1.68
	Alternative 6	50	6.16	12.2	1.92
	Alternative 6	100	6.55	12.8	2.13

### 3.0 RESULTS

IH2VOF results presented hereafter for both T-131 and R-137 include:

- Screenshots at specific times comparing the existing condition with the alternatives
- Water level,  $\eta$ , timeseries are presented and the existing condition is compared to the alternatives
- Overtopping results are presented and discussed.

#### 3.1. T-131

##### 3.1.1. Return Period Wave Results

Four screenshots are presented below representing the peak of the 15 (Figure 3-1), 25 (Figure 3-2), 50 year (Figure 3-3) and 100-year (Figure 3-4) return period storms for T-131.

- 15-Year Return Period Storm: Under existing conditions, it is possible to see the wave overtopping at the dune crest during the 15 year storm. The same wave condition does not reach the dune for Alternative 2/6. This is attributed to the rapid loss of wave energy by depth-induced breaking as waves propagate across the filled beach profile.
- 25-Year Return Period Storm: For 25 year return period, the waves also overtop the dune crest under the existing condition. The same wave condition for Alternative 2/6 only reaches the toe of the dune.
- 50-Year Return Period Storm: For both the existing conditions and Alternative 2/6, the dune crest is overtopped by waves during the 50 year storm. However, the overtopping volume is much less for Alternative 2/6.
- 100-Year Return Period Storm: The dune crest is overtopped by waves for both existing conditions and Alternative 2/6 during the 100-year storm. Alternative 2/6 shows a reduced overtopping volume compared to existing conditions.

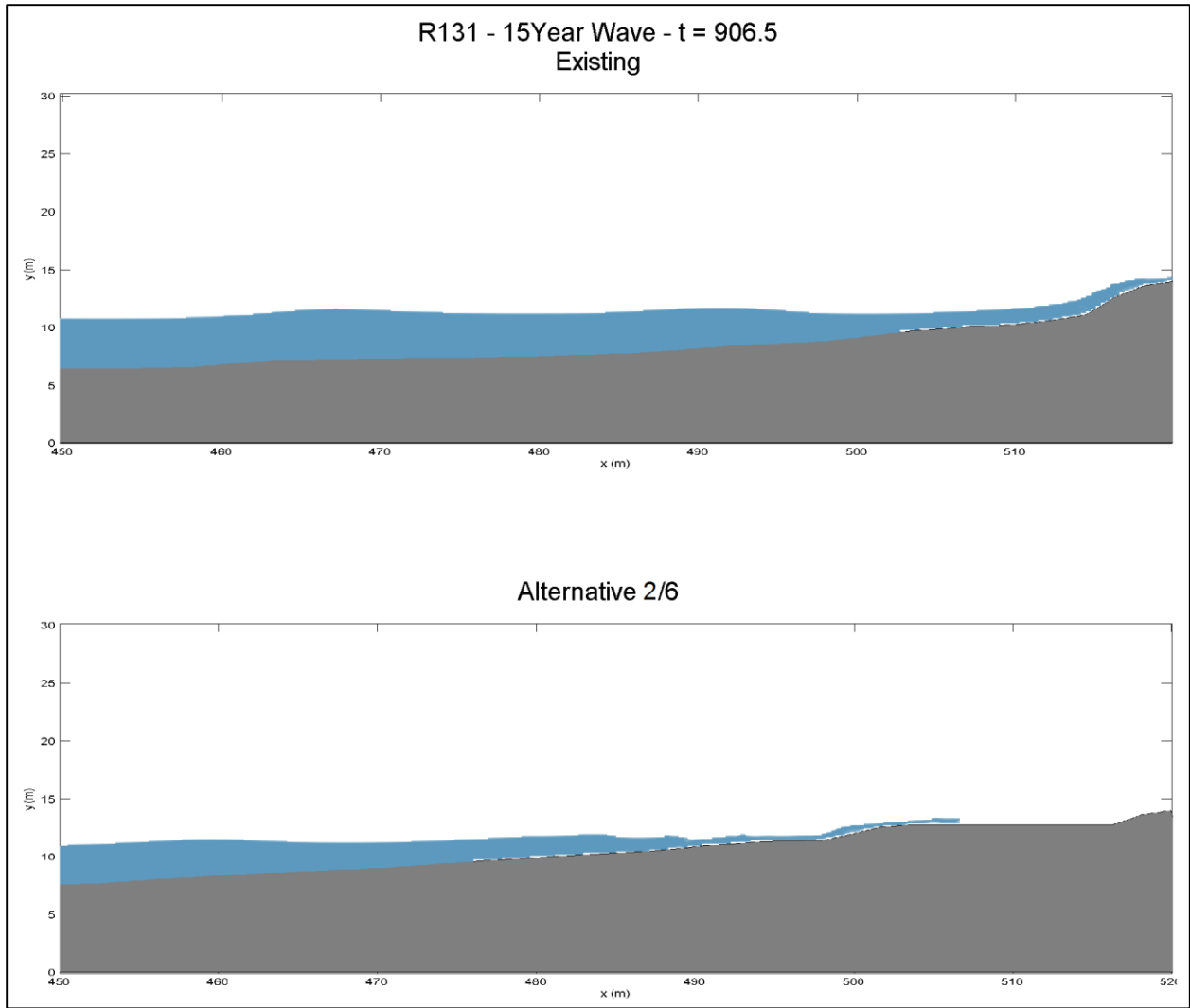
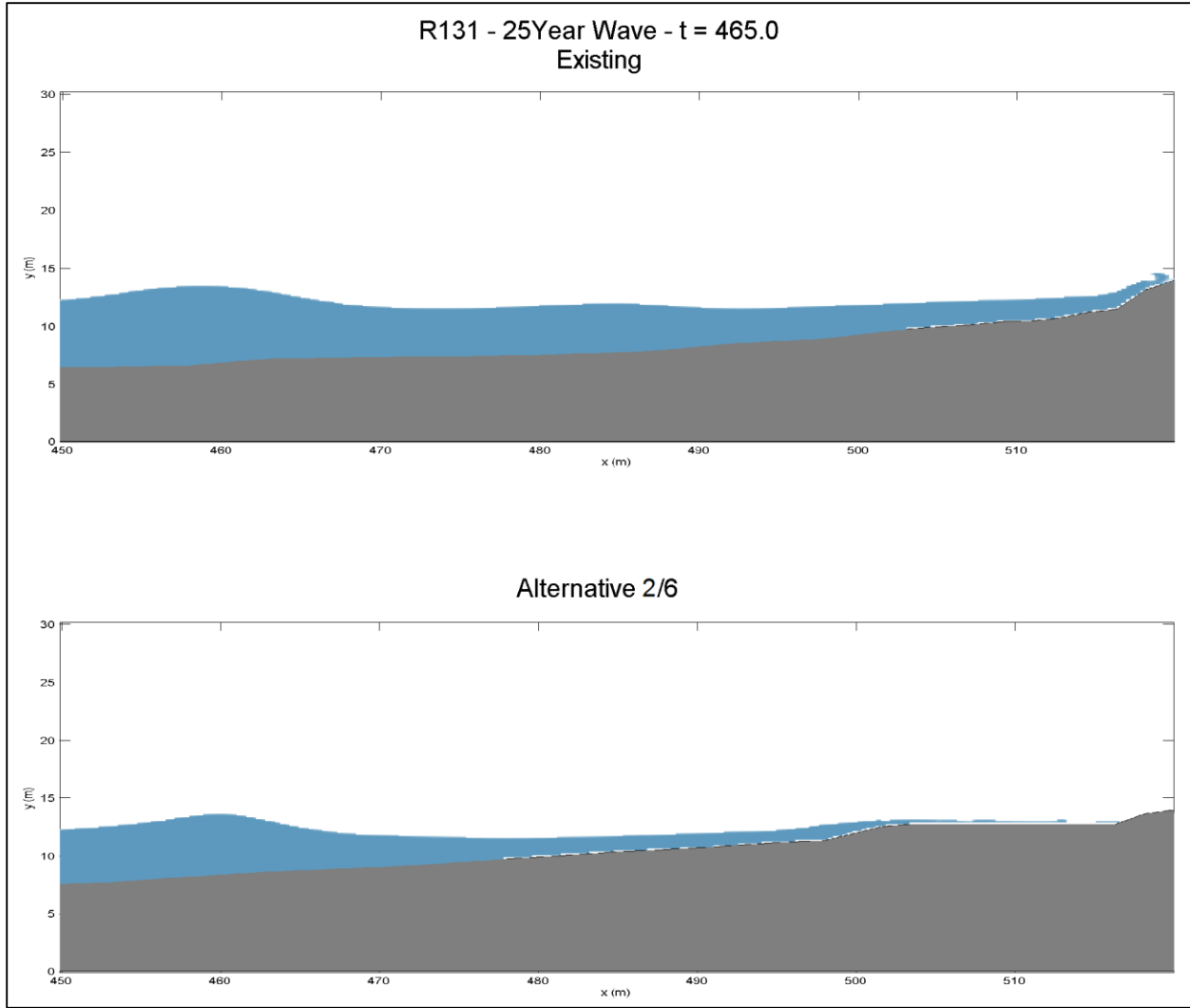
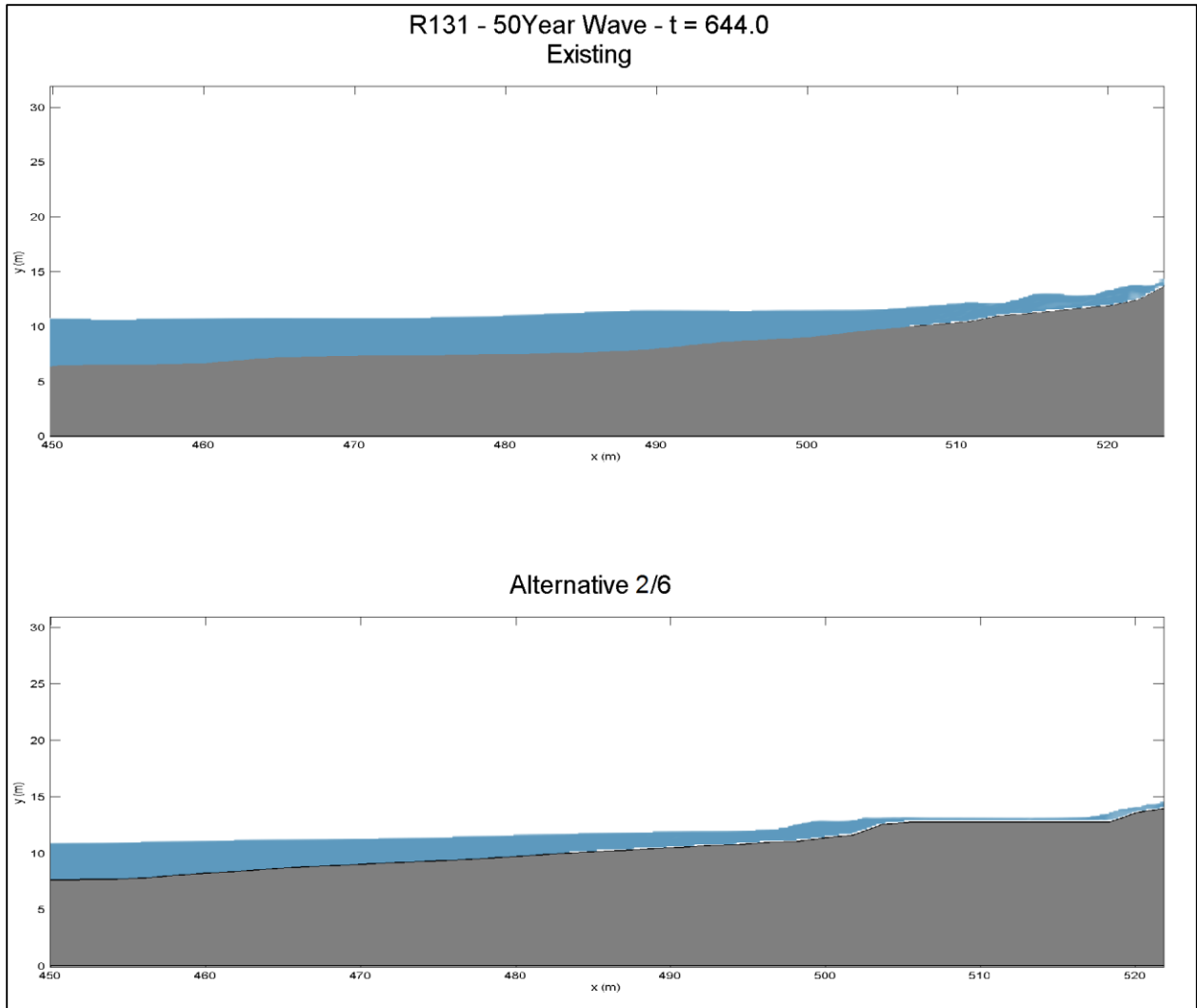


Figure 3-1. T-131 - 15 year return period wave at 906.5 s of simulation for existing (top) and Alternative 2/6 (bottom).



**Figure 3-2. T-131 - 25 year return period wave at 465 s of simulation for existing (top) and Alternative 2/6 (bottom).**



**Figure 3-3: T-131 - 50 year return period wave at 644 s of simulation for existing (top) and Alternative 2/6 (bottom).**

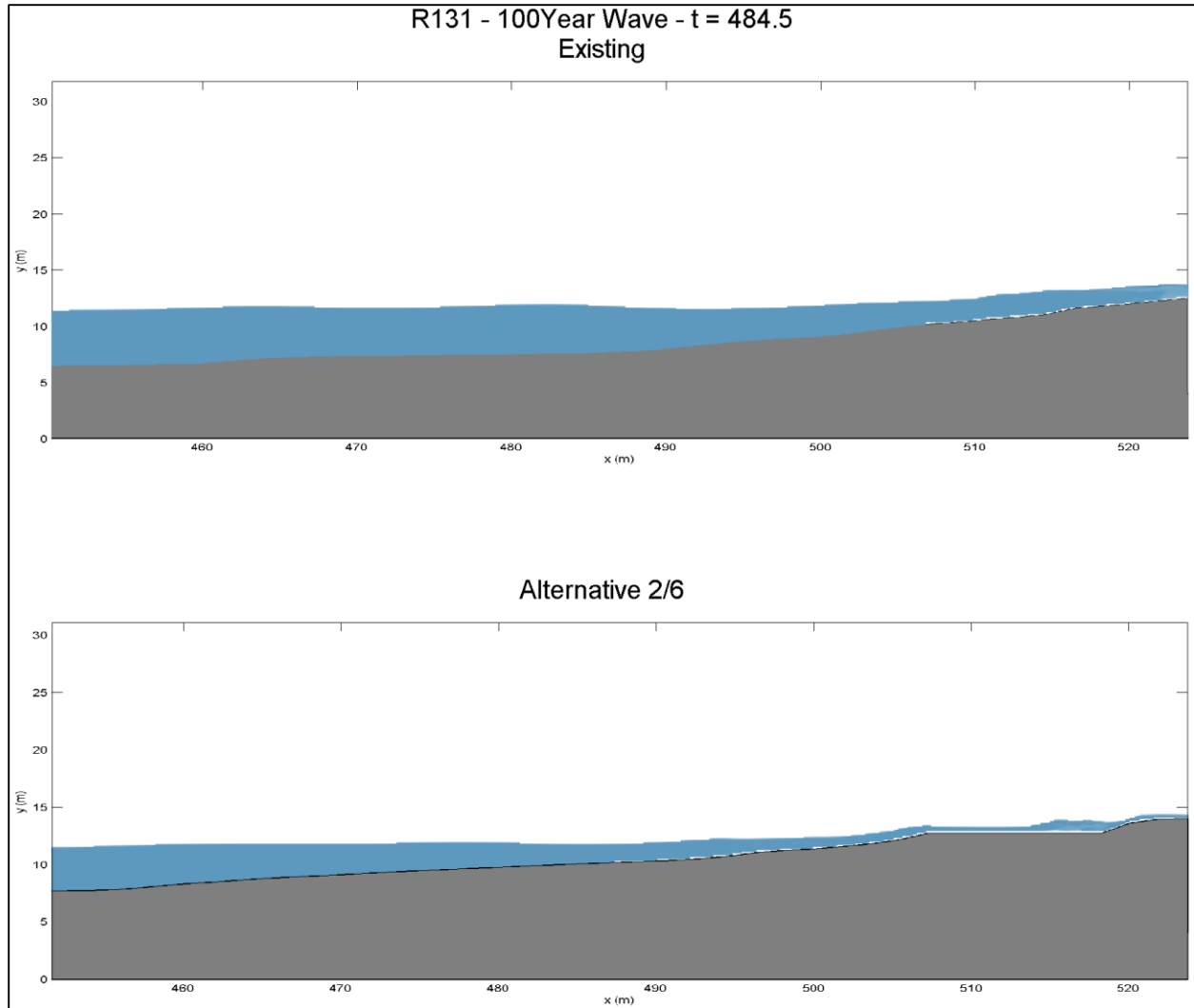


Figure 3-4: T-131 - 100 year return period wave at 484.5 s of simulation for existing (top) and Alternative 2/6 (bottom).

### 3.1.2. Probe Results

The IH2VOF models allows for “probes” to be defined in order to extract information at specific points across the beach profile. Seven probes were placed across the profile to analyze water surface ( $\eta$ ) timeseries as the wave propagates toward the beach. The results for 15- (Figure 3-5), 25- (Figure 3-6), 50- (Figure 3-7), and 100-year (Figure 3-8) return period waves are presented below for the existing conditions and the alternatives. The figures suggest that the wave height decreases across the profile from probe 1 to probe 7.

- 15 Year Return Period Storm: From probe 3 to probe 5, it is possible to observe the transfer of the energy from higher to lower frequencies due to depth-induced wave breaking. At probe 6, the presence of the beach fill from Alternatives 2/6 reduces wave energy. Overtopping of the dune crest is shown by probe 7. The thickness of water during overtopping was less than 0.5 m.
- 25 Year Return Period Storm: The 25-year return period wave is more energetic and also presents a higher water level reducing the differences between existing conditions and alternatives. The overtopping thickness at probe 7 increased to 1.0 m compared to 0.5 m for the 15-year storm.
- 50 Year Return Period Storm: The water level and wave height increase for 50 year storm, further reducing the differences between existing and alternative conditions. It should be noted that the observed water level at probe 6 is sometimes negative for existing condition. This is because the beach elevation at probe 6 is submerged for existing condition and above water for alternatives (Figure 3-7). The situation also happens in R-137 (Figure 3-15). The overtopping thickness at probe 7 increased to 1.5 m compared to 1.0 m for the 25-year storm.
- 100 Year Return Period Storm: This storm impacts beach profiles severely. The eroded beach profile together with the 100-year return period storm easily overtops the dune crest (probe 7) for existing conditions. Alternative 2/6 reduces the of wave height due to energy dissipation over the wider and shallower beach profile. As for 50 year return period storm it should be noted that the observed water level at probe 6 is sometimes negative for existing condition. This is because the beach elevation at probe 6 is submerged for existing condition and above water for alternatives. The maximum overtopping thickness at probe 7 increased to 2.4 m compared to 1.5 m for the 50-year storm.

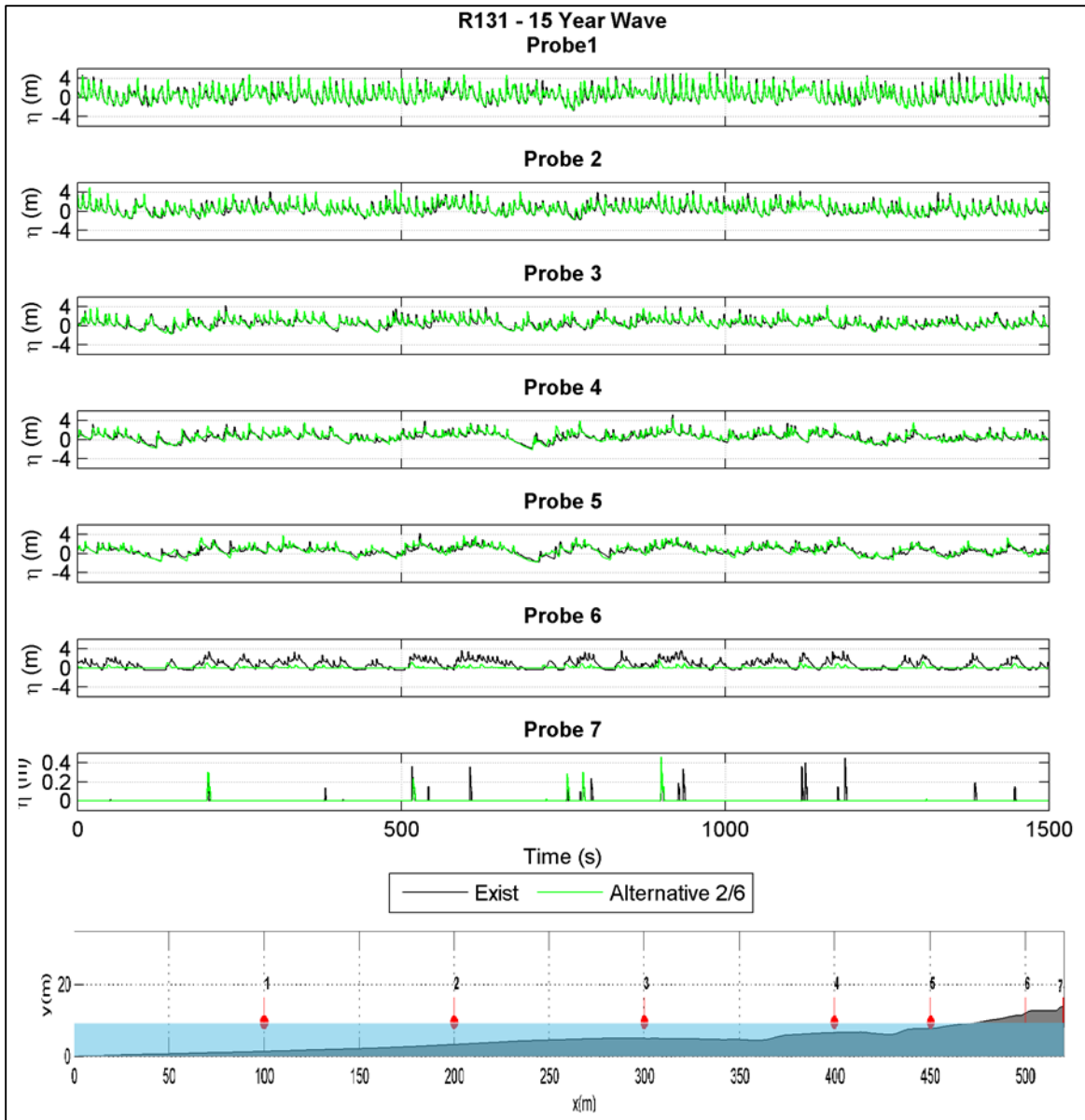


Figure 3-5. T-131 – 15-year return period wave  $\eta$  at probes 1 to 7.

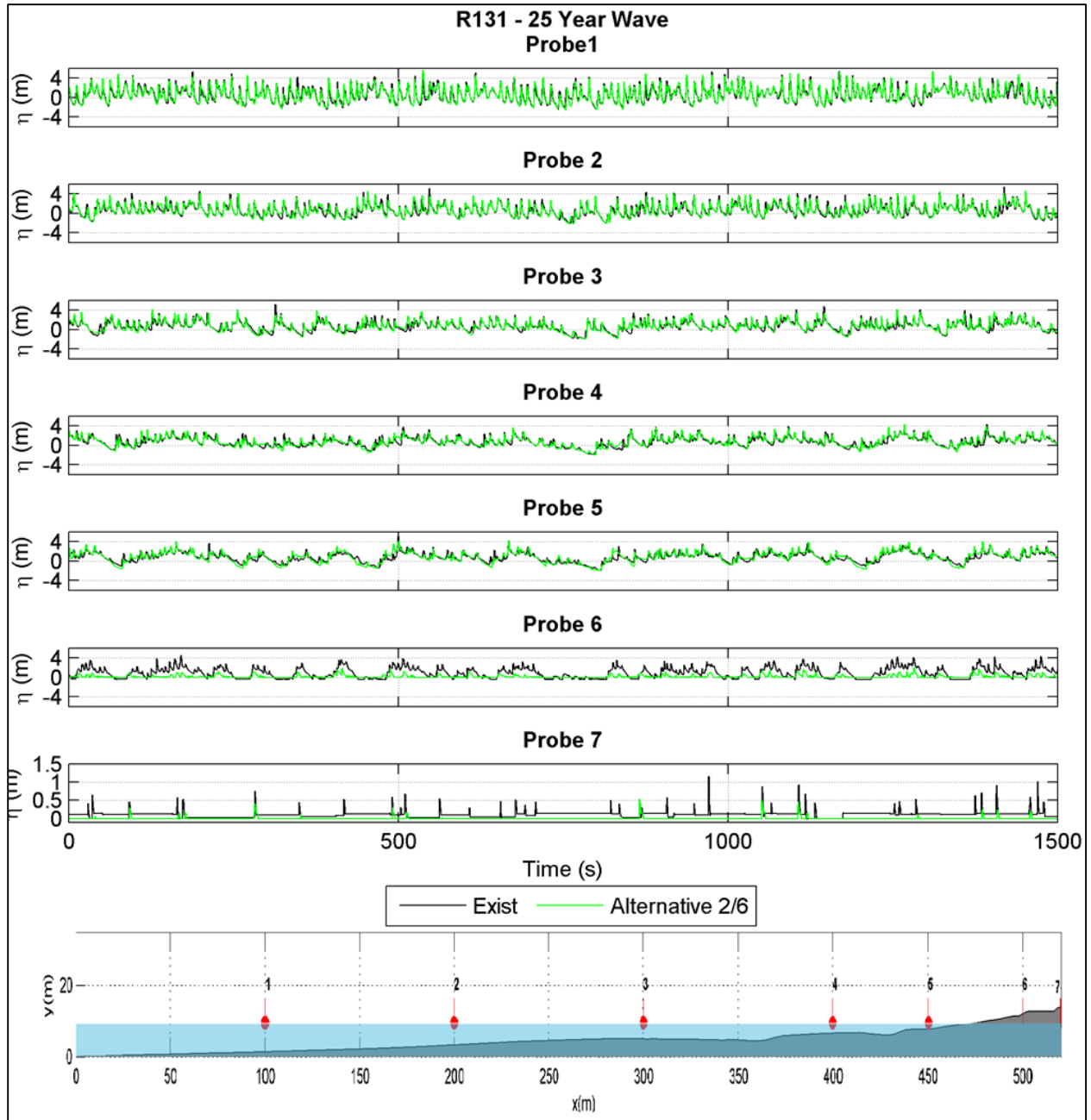


Figure 3-6. T-131 – 25-year return period wave  $\eta$  at probes 1 to 7.

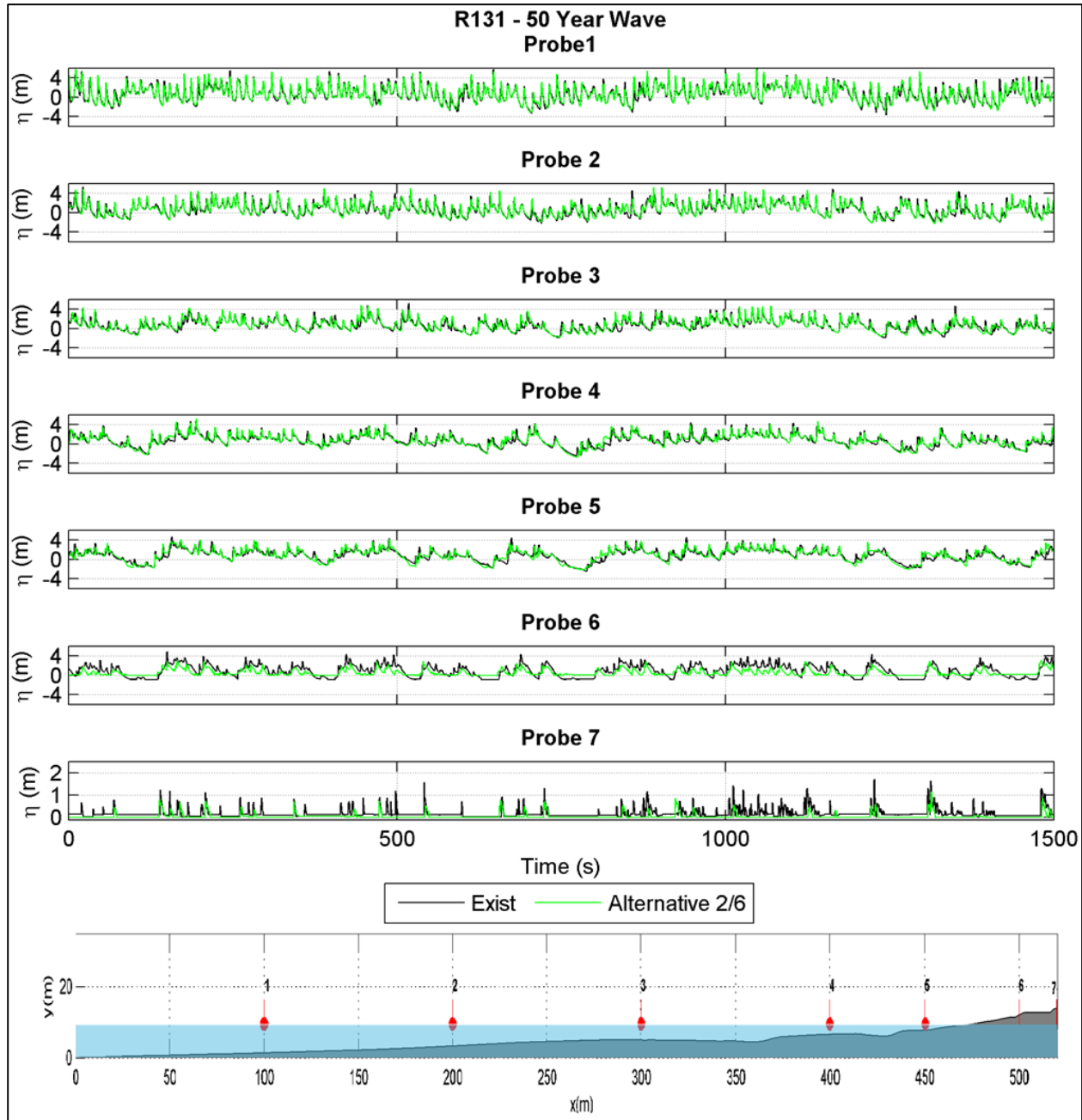


Figure 3-7. T-131 – 50-year return period wave  $\eta$  at probes 1 to 7.

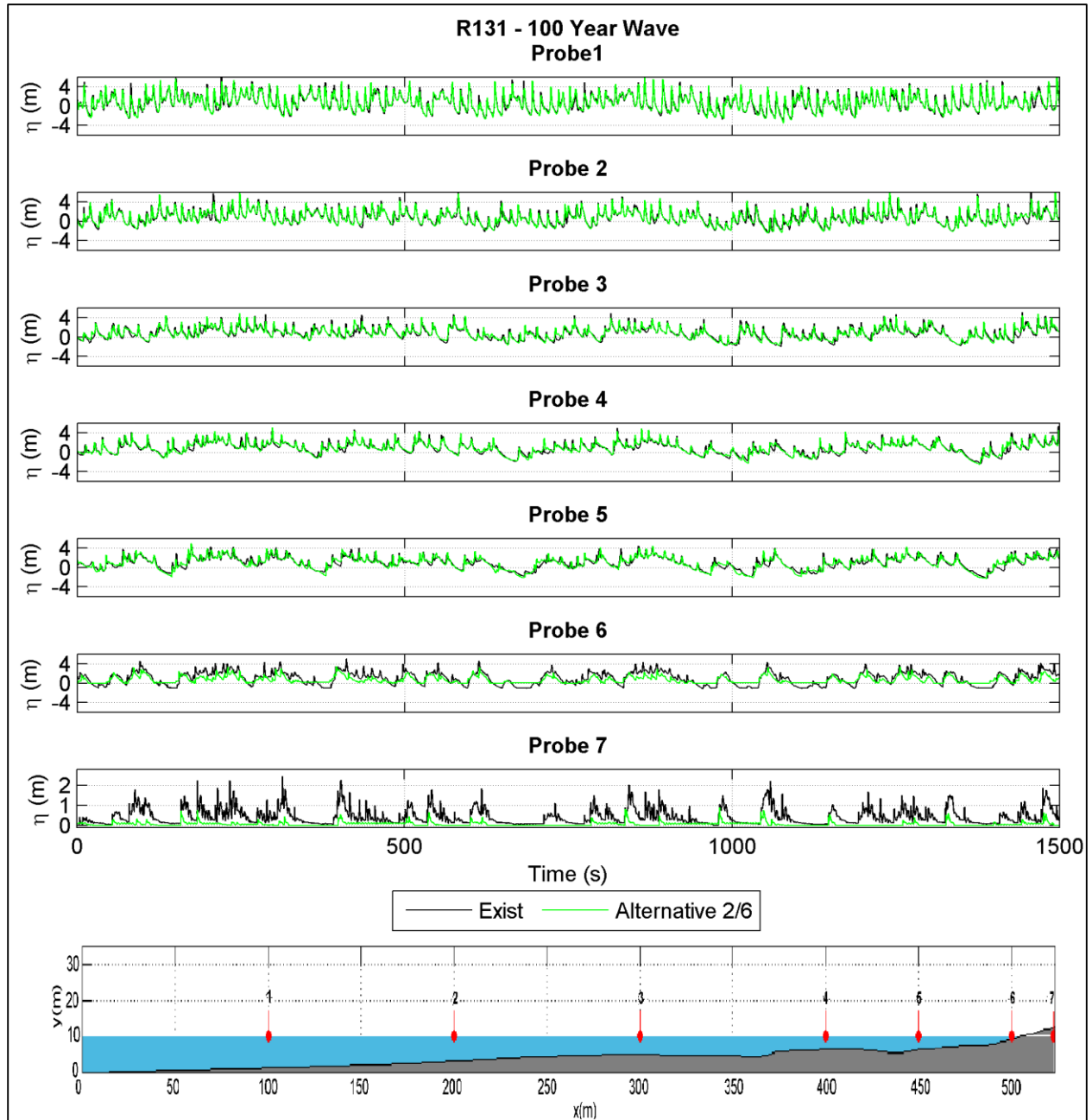


Figure 3-8. T-131 – 100-year return period wave  $\eta$  at probes 1 to 7.

### 3.1.3. Dune Overtopping Results

The dune overtopping results are shown below for 15 (Figure 3-9), 25 (Figure 3-10), 50 (Figure 3-11) and 100 (Figure 3-12) year return period waves. The alternatives reduce wave energy as they propagate over the beach profile and consequently, yield less overtopping than the existing conditions. Due to the randomness of generated waves, the instantaneous overtopping values for the alternatives such as the maximum overtopping volume can be larger than the existing conditions. However, the cumulative or mean overtopping values are less with the alternatives.

- 15-Year Return Period Storm: The overtopping thickness was lower than 0.5 m. The mean overtopping velocity can reach 6.48 and 5.53 m/s for existing conditions and alternatives, respectively. The instantaneous overtopping volume (volume overtopped by one wave) can reach 5 m<sup>3</sup>/m for the existing conditions and alternatives. The mean overtopping discharge for existing and alternative conditions was 0.03 and 0.01 m<sup>3</sup>/s/m, respectively. This equates to a 67% reduction in overtopping with the alternatives. It should be noted that during the first 500 seconds of the simulation (Figure 3-9) the cumulative overtopping volume for the alternatives exceeded the existing condition, which was attributed to the randomness of generated waves. Over the entire simulation period, the cumulative overtopping volume for the alternatives was less than the existing condition.
- 25-Year Return Period Storm: The results showed an overtopping thickness with an order of magnitude of 1 m. The mean overtopping discharge was reduced by 75% from 0.08 m<sup>3</sup>/m/s under existing conditions to 0.02 m<sup>3</sup>/m/s for the alternatives. The maximum overtopping volumes were similar ranging from 9.71 to 9.99 m<sup>3</sup>/m for the existing conditions and the alternatives. The maximum overtopping velocities were reduced from 8.59 m/s to 7.76 m/s for the existing conditions and the alternatives, respectively.
- 50-Year Return Period Storm: The results showed an overtopping thickness with an order of magnitude of 1.5 m. There was a 58% reduction of mean overtopping

discharge from 0.31 to 0.13 m<sup>3</sup>/s/m for the existing conditions and alternatives, respectively. The maximum overtopping volume were similar increasing from 22.54 m<sup>3</sup>/m to 23.61 m<sup>3</sup>/m and the maximum overtopping velocity was reduced from 10.18 m/s to 8.59 m/s for the existing conditions and alternatives, respectively.

- 100-Year Return Period Storm: The overtopping thickness presented an order of magnitude of 2.4 m. The mean overtopping discharge decreased 69% comparing the existing condition and the alternative 2/6 (from 0.77 to 0.24 m<sup>3</sup>/s/m). The maximum overtopping volume decreased 46% from 85.04 (existing) to 45.67 m<sup>3</sup>/m (Alternative 2/6). The maximum overtopping velocity was reduced from 10.76 m/s to 8.86 m/s for the existing conditions and alternatives, respectively (corresponding to 18%).

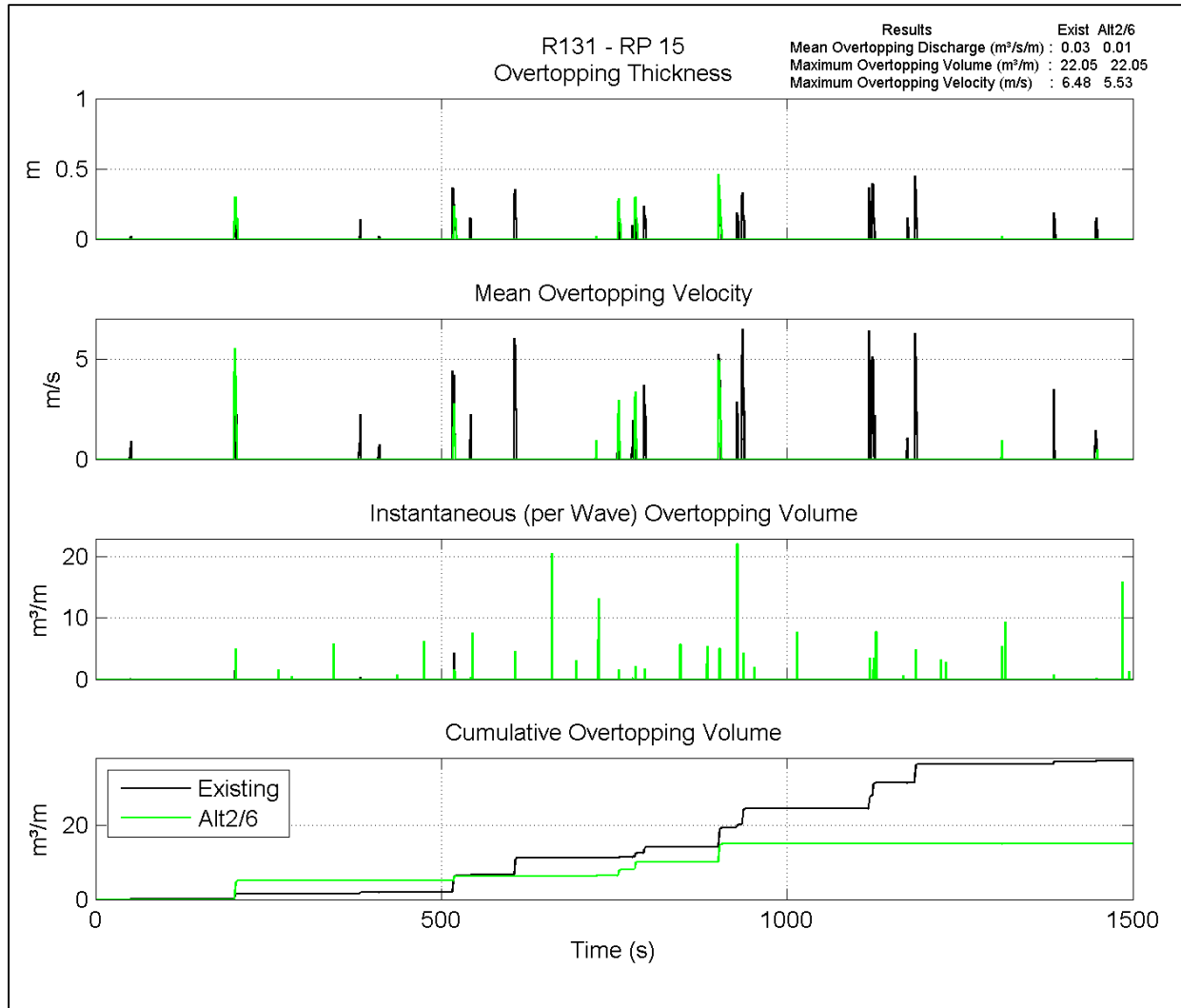


**Figure 3-9. Overtopping results - T-131 – 15-year return period for existing conditions (black) and with alternative (green).**

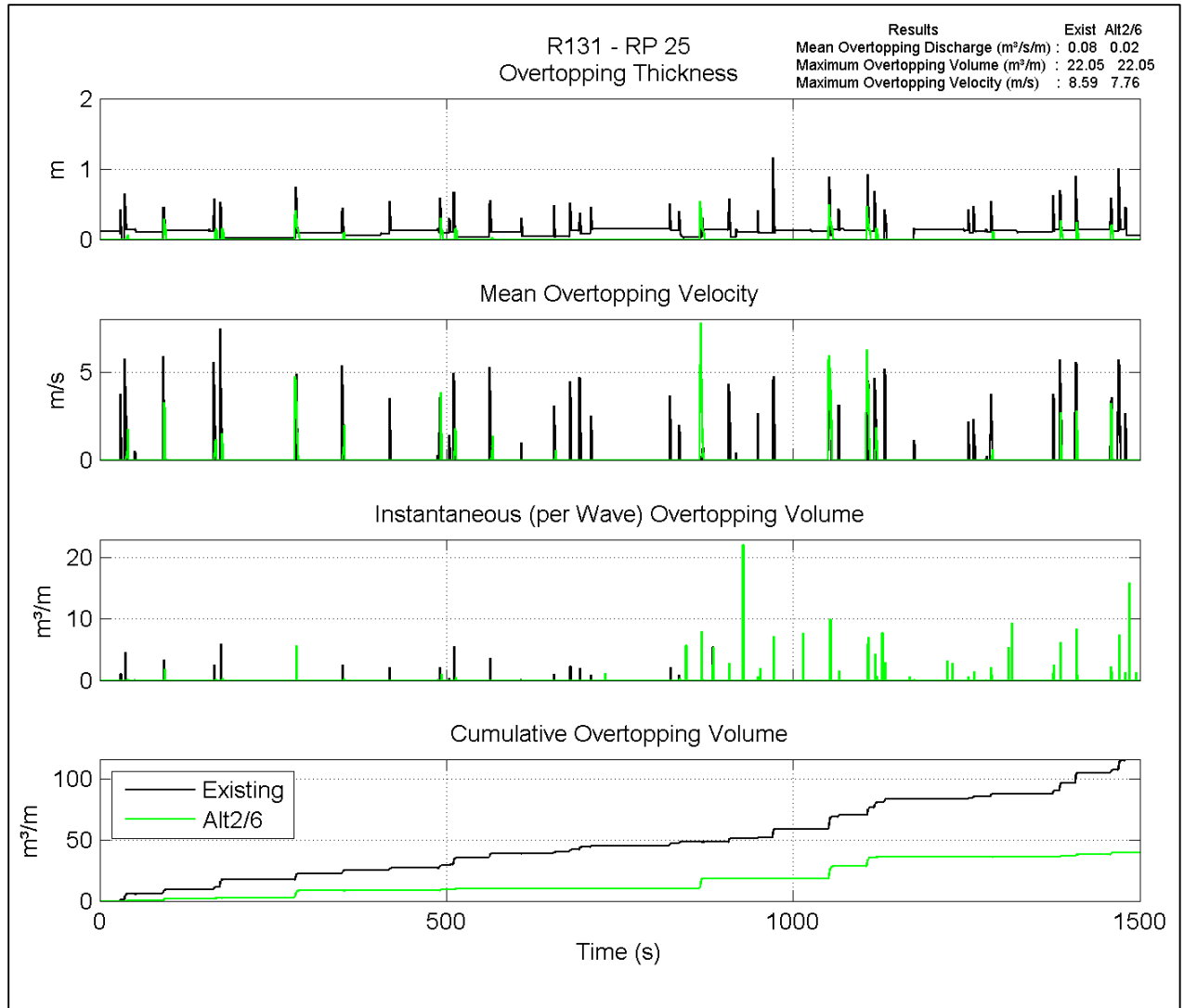


**Figure 3-10. Overtopping results - T-131 – 25-year return period for existing conditions (black) and with alternative (green).**

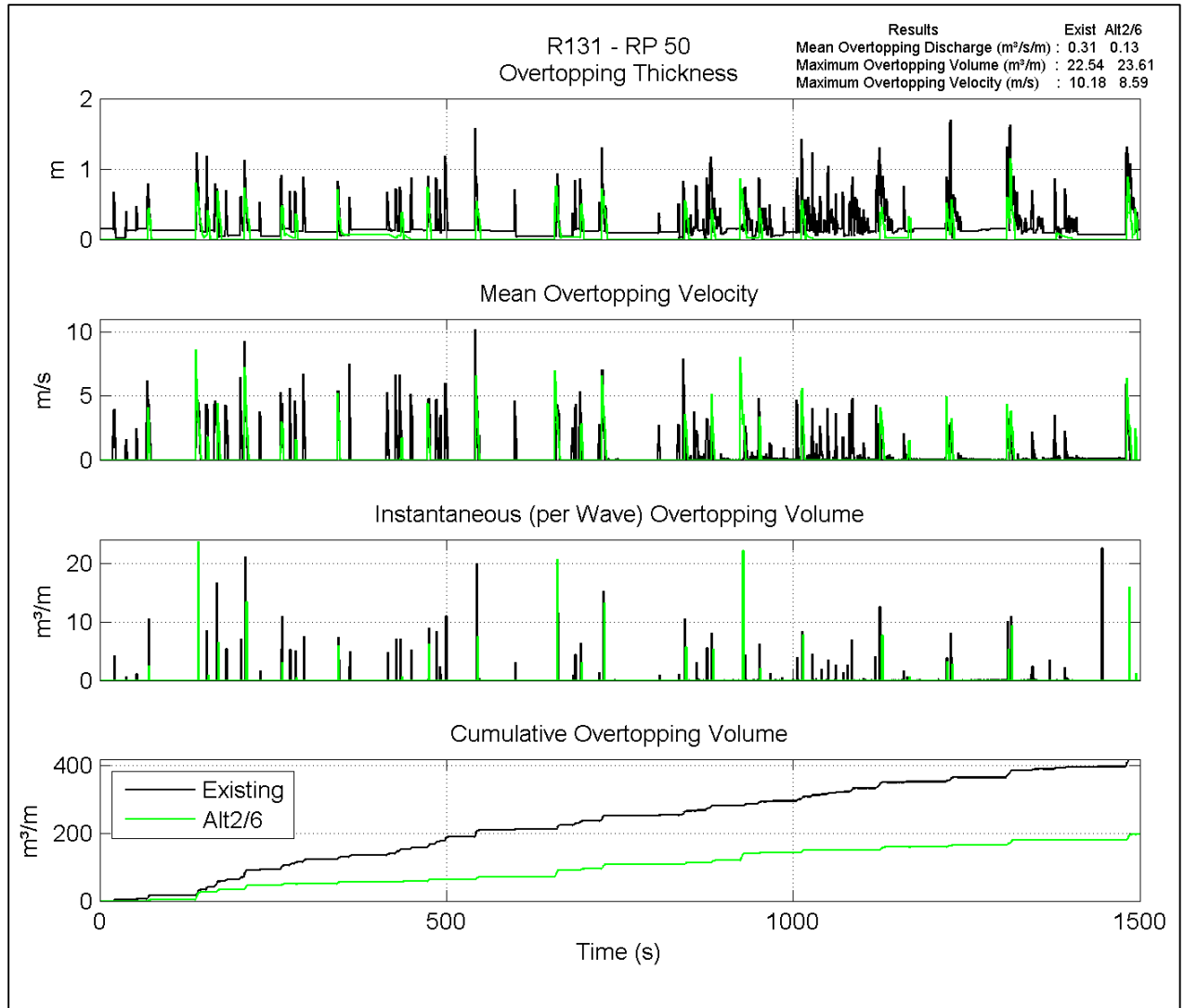


**Figure 3-11. Overtopping results - T-131 – 50-year return period for existing conditions (black) and with alternative (green).**

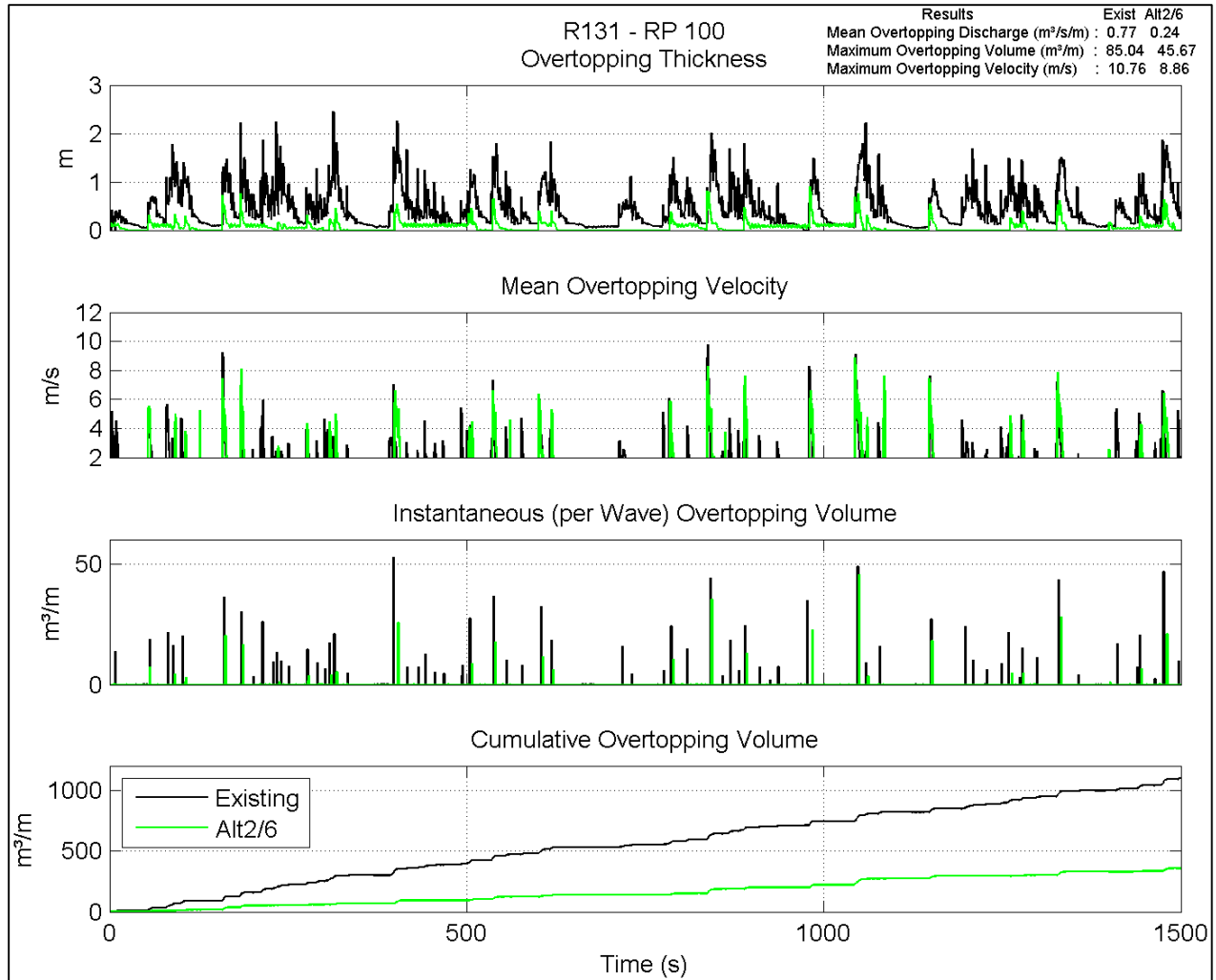


**Figure 3-12. Overtopping results - T-131 – 100-year return period for existing conditions (black) and with alternative (green).**

### 3.2. R-137

The variations in water levels and overtopping for which a seawall is in place are presented below for the existing conditions, Alternative 2, and Alternative 6 are presented below. Unlike the beach fill at T-131, the fill volume at R-137 for Alternative 6 was greater than the volume for Alternative 2.

#### 3.2.1. Return Period Wave Results

Screenshots of simulations at R-137 during the peak of the storms are shown in Figure 3-13 through Figure 3-16.

- 15-Year Return Period Storm: Waves overtopped the dune crest for existing conditions. Waves reached but did not overtop the dune crest for Alternative 2, while the waves did not reach the dune for Alternative 6.
- 25-Year Return Period Storm: Waves overtopped the dune crest for the existing conditions and Alternative 2, while overtopping was not evident with Alternative 6.
- 50-Year Return Period Storm: The dune crest was overtopped for all scenarios, but there was less overtopping with the alternatives.
- 100-Year Return Period Storm: As for 50-year return period storm, the dune crest was overtopped for all 100 year return period storm scenarios, but there was less overtopping with the alternatives.

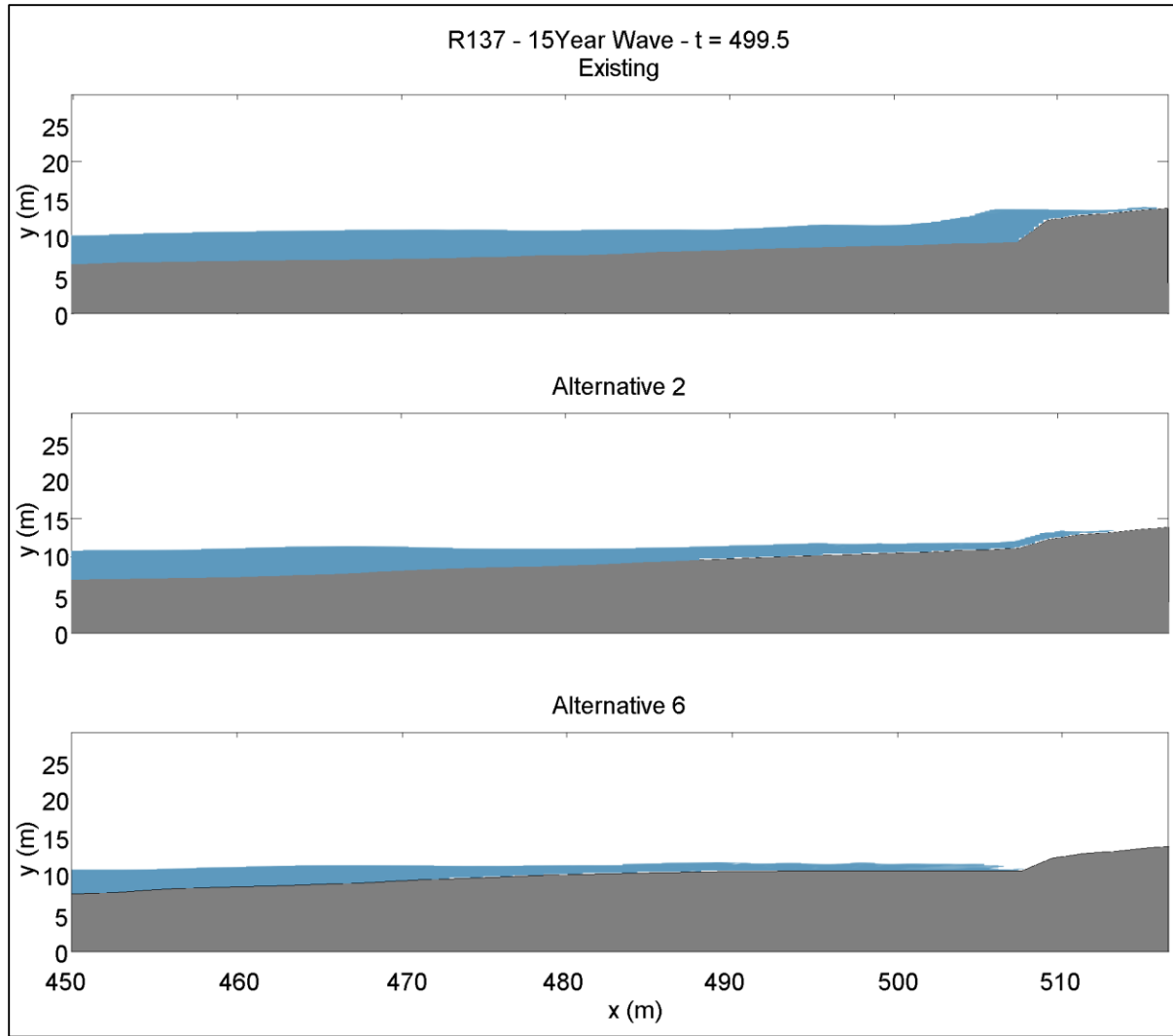


Figure 3-13. R-137 – 15-year return period wave at 499.4 s of simulation for existing (top), Alternative 2 (centre) and Alternative 6 (bottom).

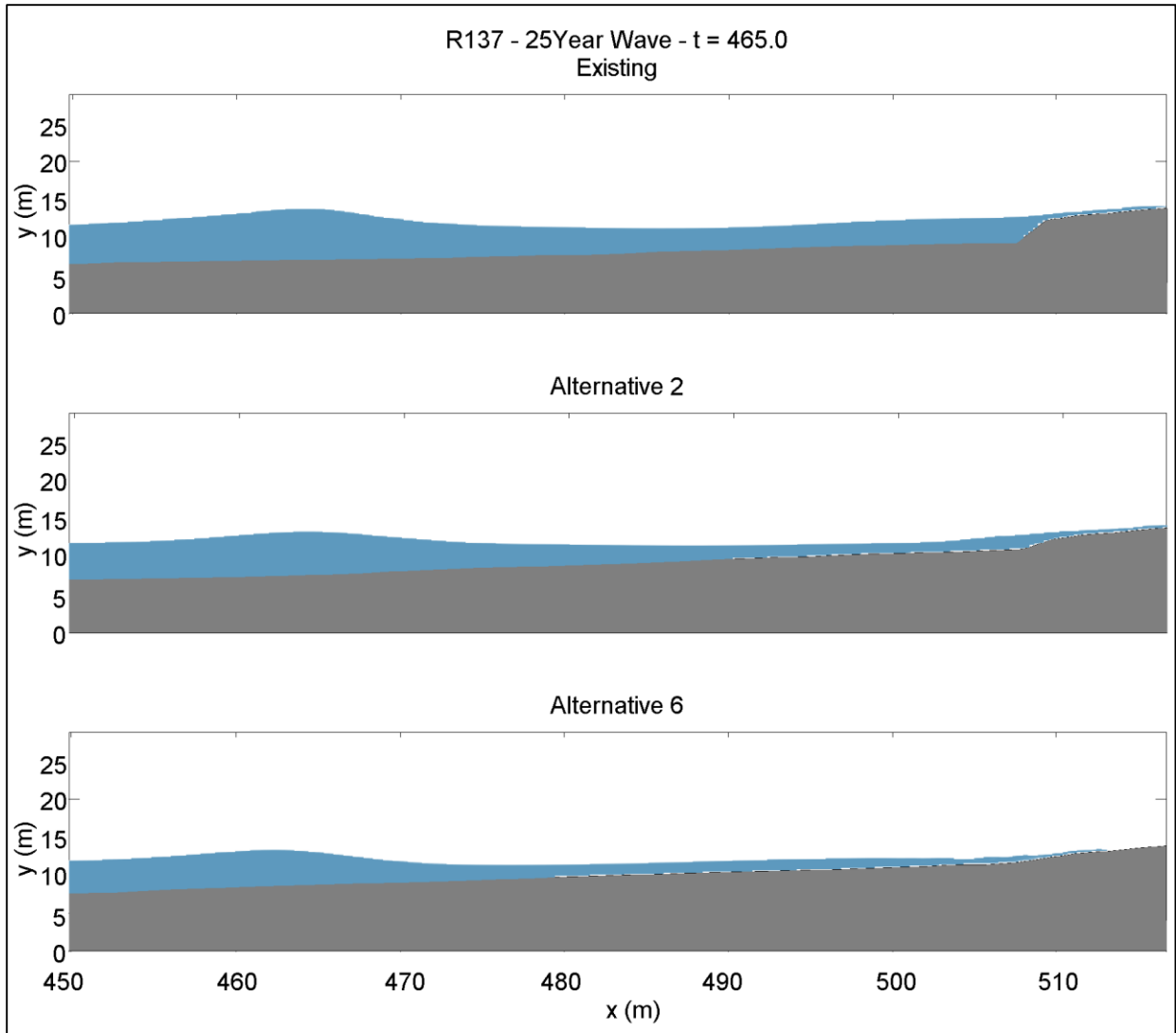


Figure 3-14 R-137 – 25-year return period wave at 465 s of simulation for existing (top), Alternative 2 (centre) and Alternative 6 (bottom).

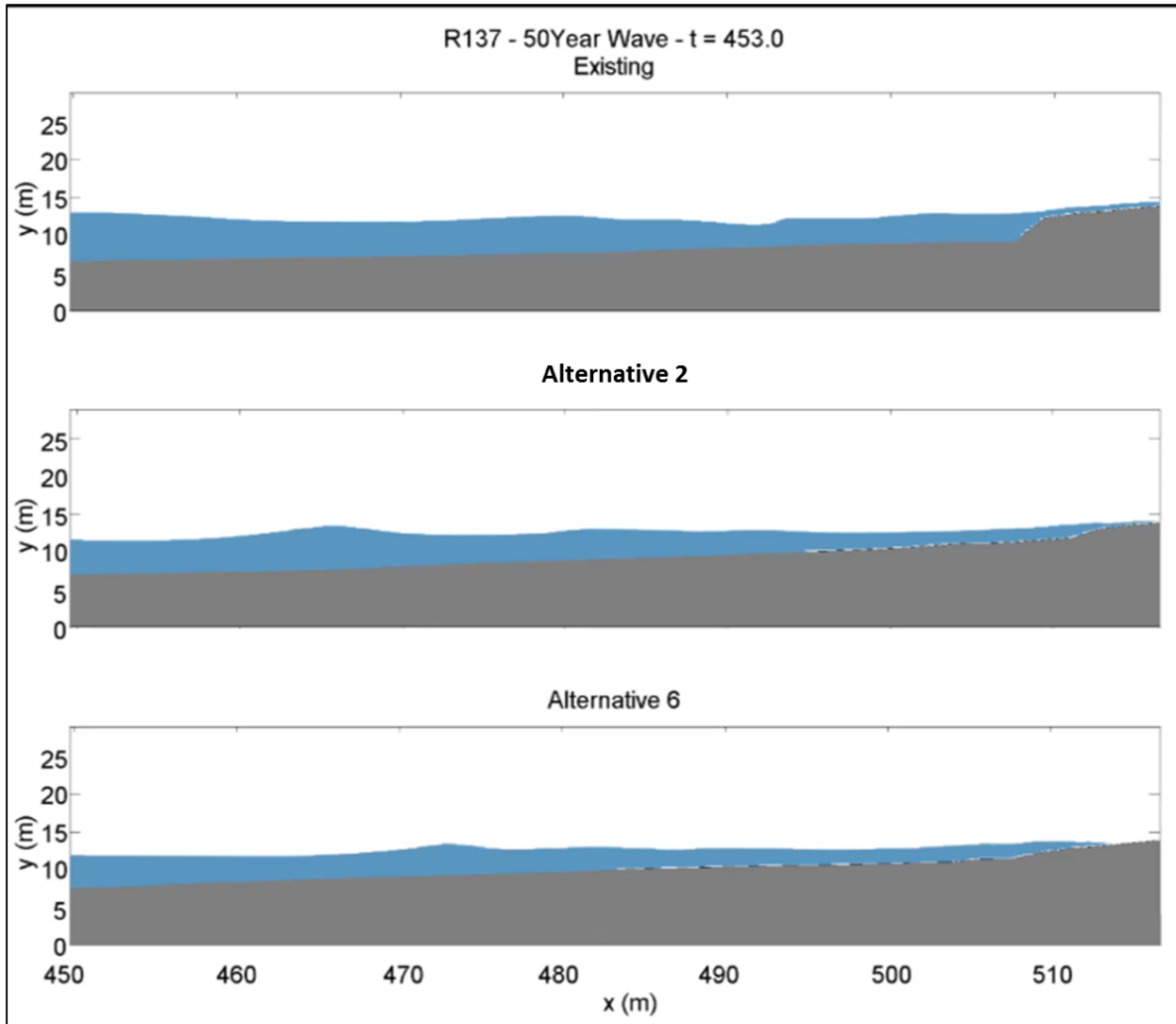
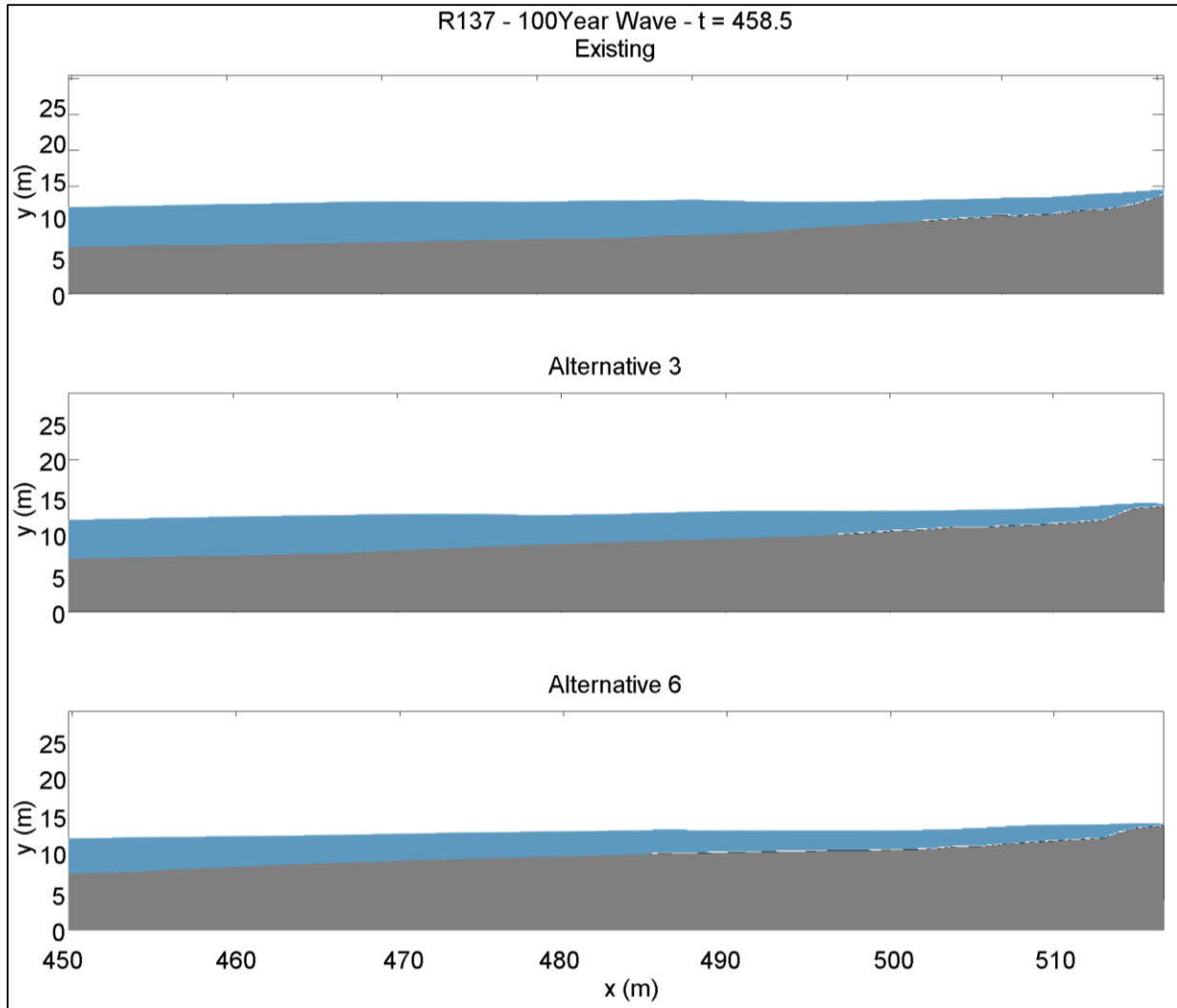


Figure 3-15. R-137 – 50-year return period wave at 440 s of simulation for existing (top), Alternative 2 (centre) and Alternative 6 (bottom).



**Figure 3-16. R-137 – 100-year return period wave at 458.5 s of simulation for existing (top), Alternative 2 (centre) and Alternative 6 (bottom).**

### 3.2.2. Probe Results

Similar to the analysis for T-131, seven probes were placed along the beach profile in order to analyze water surface ( $\eta$ ) timeseries as the wave propagates toward the beach. The results for 15- (Figure 3-17), 25- (Figure 3-18), 50- (Figure 3-19) and 100-year (Figure 3-20) return period waves are presented below to compare the existing conditions, Alternative 2 and Alternative 6. The figures indicate a reduction in wave height as the waves propagate toward the coast. From probe 4 to probe 6, the wave energy transfers from higher to lower frequencies due to wave breaking, similar to that observed at T-131. At probe 6, the beach nourishment on wave propagation as the wave height is reduced with the alternatives as compared to the existing conditions.

- 15-Year Return Period Storm: The  $\eta$  timeseries for existing conditions presented much higher range than alternative condition, especially for 15-year return period wave. Probe 7 indicates the overtopping thickness for 15-year return period was 0.6 m.
- 25-Year Return Period Storm: The 25-year wave is more energetic and also presents a higher water level, which reduces the differences between existing and alternative conditions. Probe 7 indicates the overtopping thickness for 25-year return period was 0.8 m.
- 50-Year Return Period Storm: For 50-year return period waves, the water level is even higher, and waves reached probe 7 more frequently and the differences between existing and alternative conditions are lower. From probe 7, it is possible to see the thickness of water overtopping the dune crest. The overtopping thickness for 50 year return period was 1.2 m. For the same wave condition at probe 6 it is possible to observe that for existing condition the wave runs down and can be below sea level several times during the simulation. On the other hand, for Alternative 6, the probe is located at dry beach and it will not present values lower than zero.

- 100-Year Return Period Storm: For 100 year return period waves, the water level is the highest, and waves reached probe 7 during most of the simulated period. The dune crest is overtopped in all scenarios although differences between existing and alternative conditions are observed. The overtopping thickness for 100 year return period was almost 3 m (probe 7).

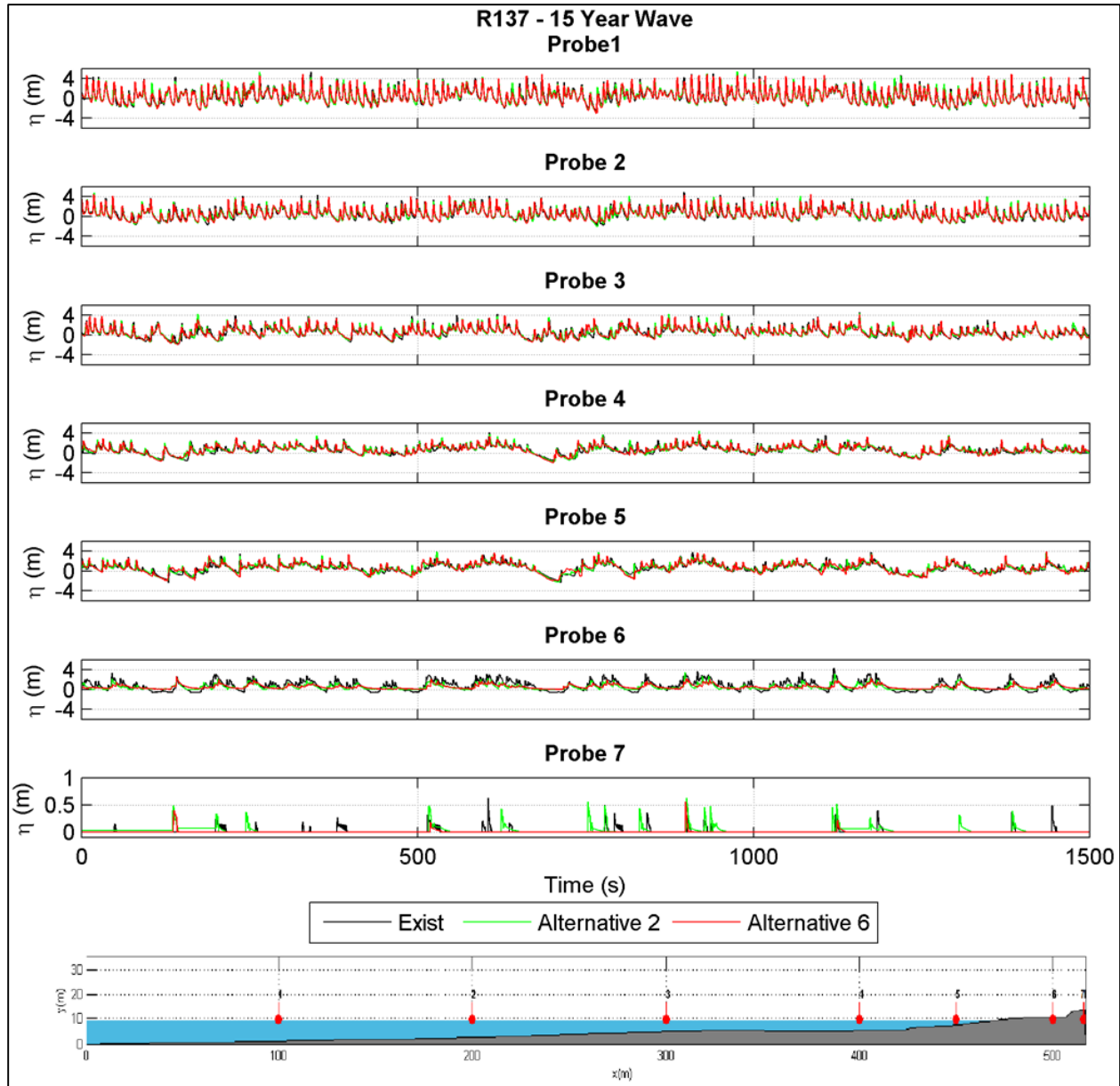


Figure 3-17. R-137 – 15-year return period wave  $\eta$  at probes 1 to 7.

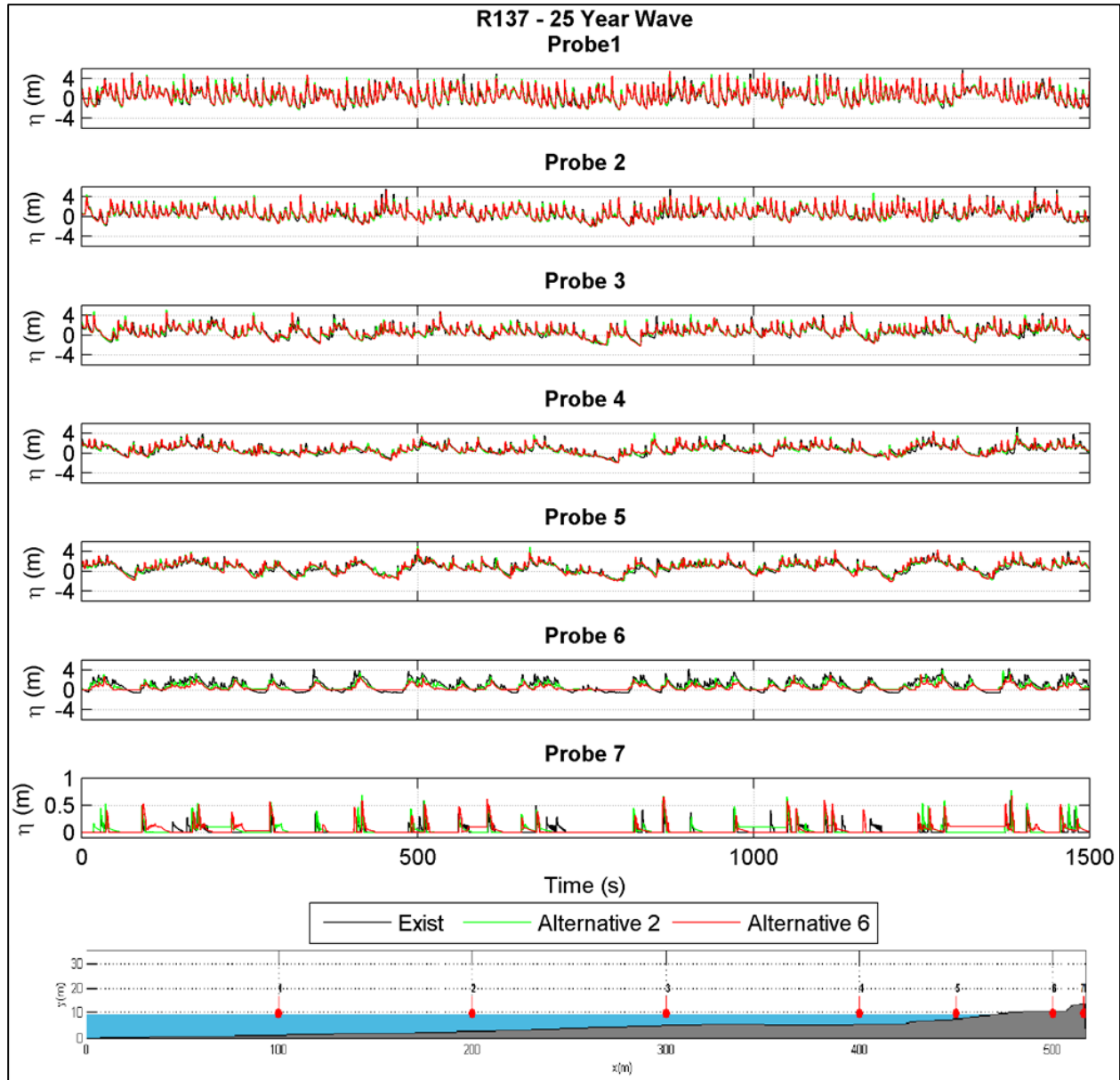


Figure 3-18. R-137 – 25-year return period wave  $\eta$  at probes 1 to 7.

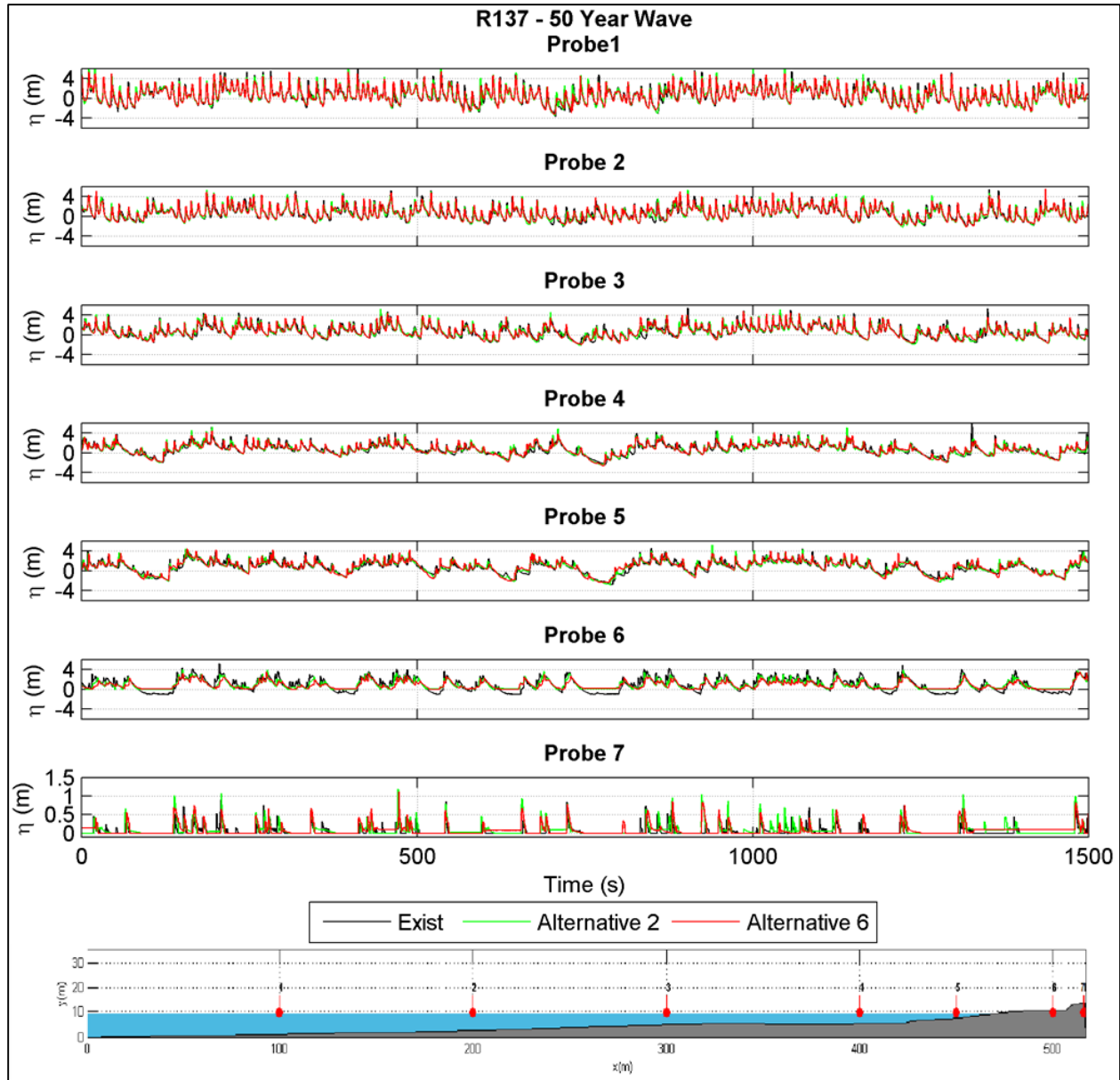


Figure 3-19. R-137 – 50-year return period wave  $\eta$  at probes 1 to 7.

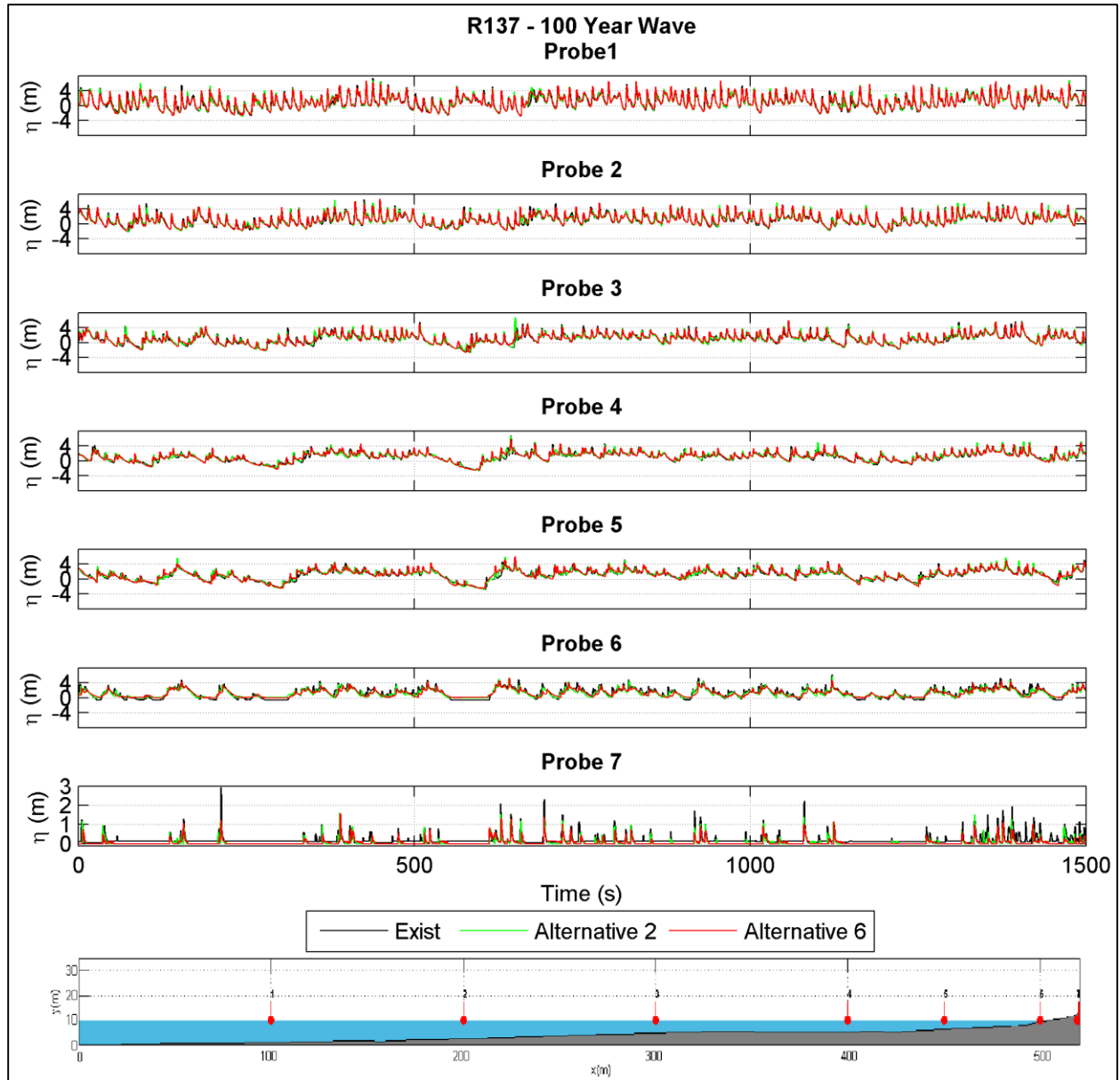


Figure 3-20. R-137 – 100-year return period wave  $\eta$  at probes 1 to 7.

### 3.2.3. Dune Overtopping Results

The dune/seawall overtopping results are shown below for 15- (Figure 3-21), 25- (Figure 3-22), 50- (Figure 3-23) and 100-year (Figure 3-24) return period waves. All the results show that presence of the alternatives reduced the wave energy propagating across the beach profile and consequently the overtopping the dune crest.

- **15-Year Return Period Storm:** The overtopping thickness is about 0.6 m for the existing conditions. Alternative 6 was considerably more effective to avoid overtopping than existing conditions and Alternative 2. The mean overtopping velocity can reach 9.67 (existing), 6.68 (Alternative 2) and 4.87 m/s (Alternative 6). The mean overtopping discharge for existing conditions, Alternative 2, and Alternative 6 was 0.04, and 0.03 and <0.01 m<sup>3</sup>/s/m, respectively. That represents a reduction of 25% for Alternative 2 and over 88% for Alternative 6 as compared to the existing conditions. The cumulative overtopping volume for Alternative 6 is less than the existing conditions indicating a reduction in the frequency that the dune crest is overtopped. The cumulative overtopping volume for Alternative 2 does not reduce the cumulative overtopping volume significantly from existing condition.
- **25-Year Return Period Storm:** The results showed an overtopping thickness of about 0.8 m for the exiting conditions. A mean overtopping discharge of 0.09 (existing conditions), 0.09 (Alternative 2) and 0.07 (Alternative 6) m<sup>3</sup>/m/s was observed. Alternative 2 showed no improvement, while Alternative 6 resulted in a 22% reduction in the overtopping discharge as compared to the existing conditions.
- **50-Year Return Period Storm:** The results showed an overtopping thickness of almost 1.5 m. For this case, the mean overtopping discharge calculated was 0.25, 0.23 and 0.21 for the existing conditions, Alternative 2 and Alternative 6, respectively. This represented a reduction of 8% for Alternative 2 and 16% for Alternative 6.

- 100-Year Return Period Storm:** The results showed an overtopping thickness close to 3 m. The mean overtopping discharge calculated for this storm case was 0.53 (existing), 0.48 (Alternative 2) and 0.21 (Alternative 6) m<sup>3</sup>/s/m. This represented a reduction of 9% for Alternative 2 and 19% for Alternative 6.

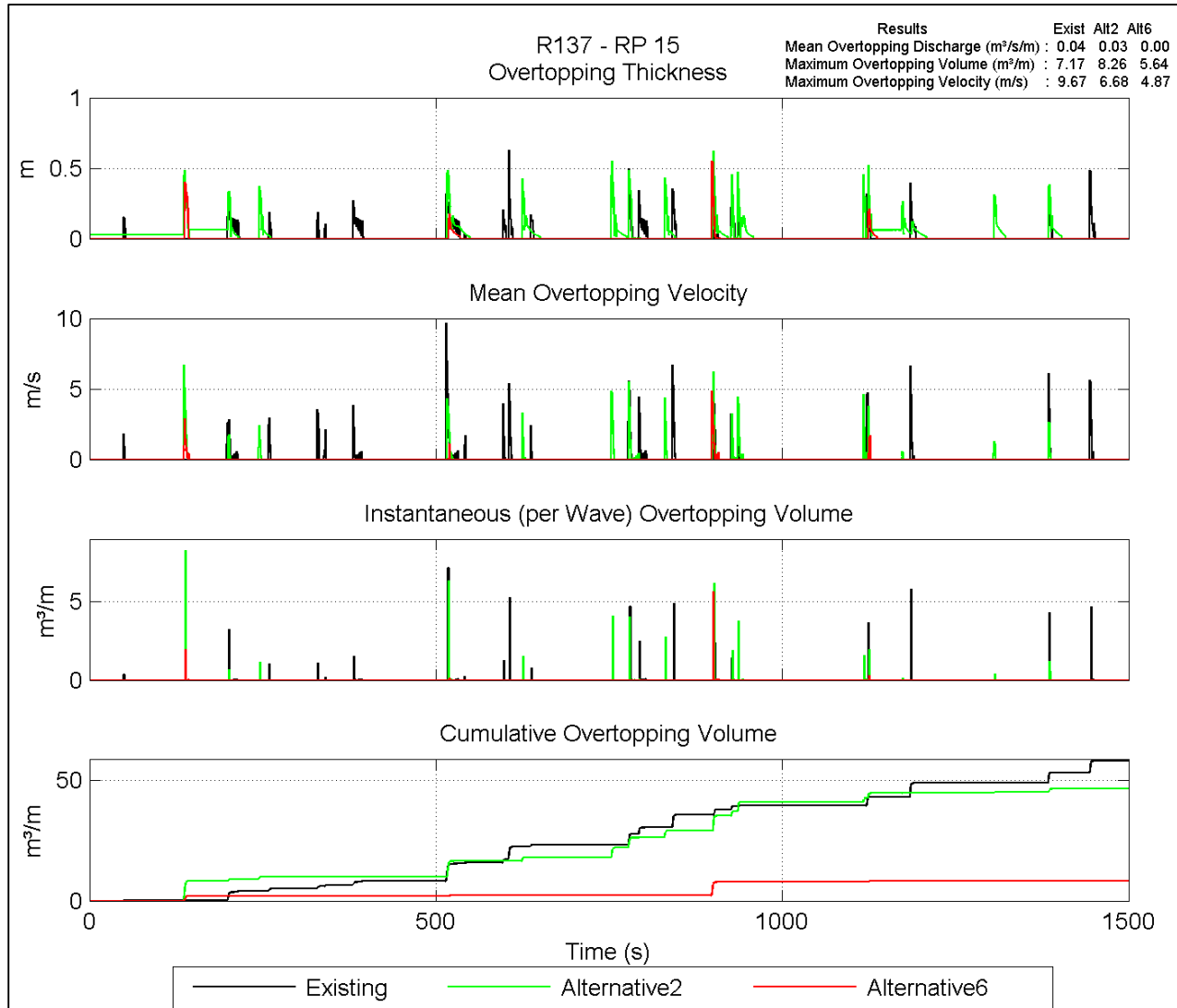


**Figure 3-21. Overtopping results - R-137 – 15-year return period for existing conditions (black), Alternative 2 (green), Alternative 6 (red).**

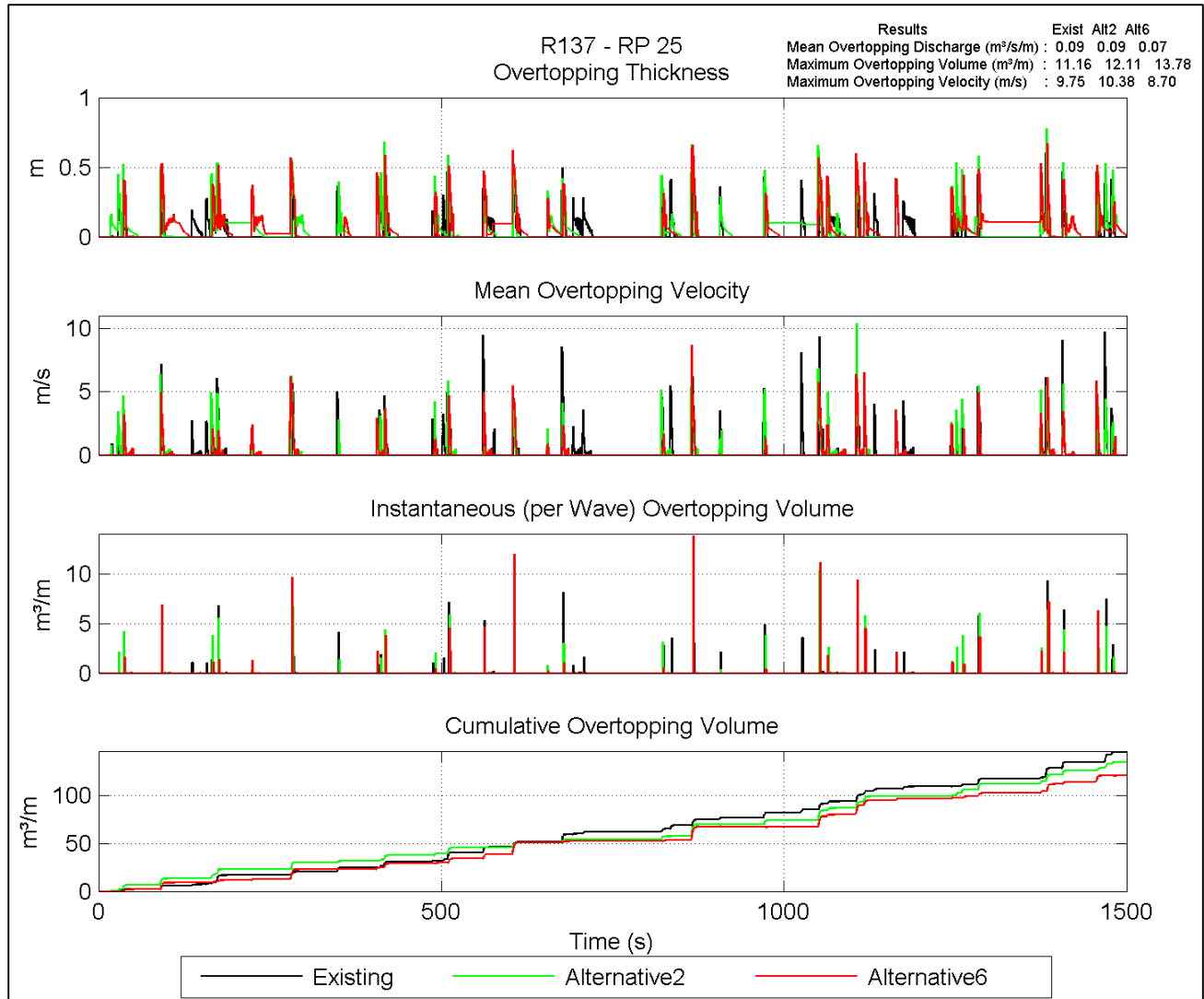


**Figure 3-22. Overtopping results - R-137 – 25-year return period for existing conditions (black), Alternative 2 (green), Alternative 6 (red).**

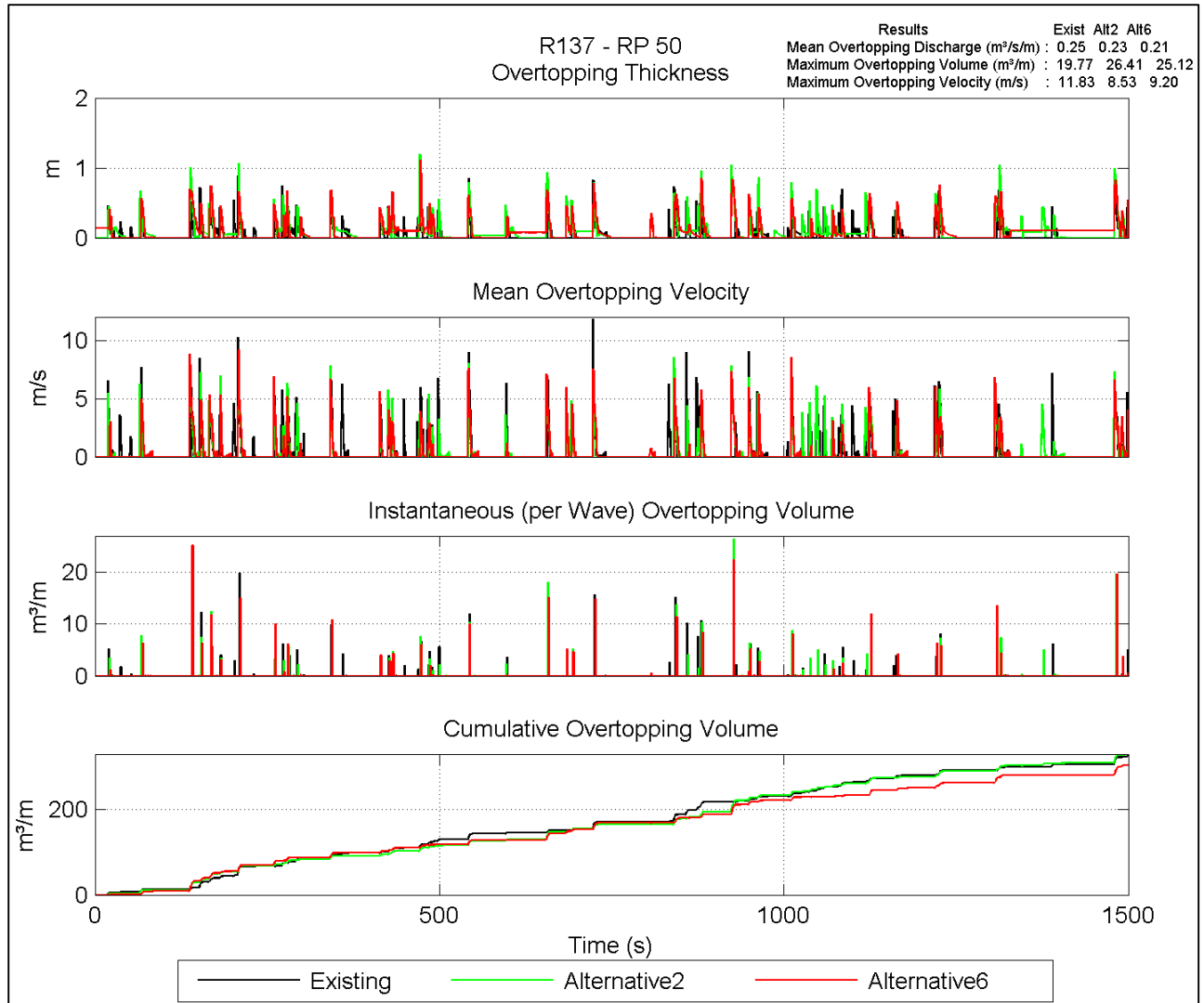


**Figure 3-23. Overtopping results - R-137 – 50-year return period for existing conditions (black), Alternative 2 (green), Alternative 6 (red).**

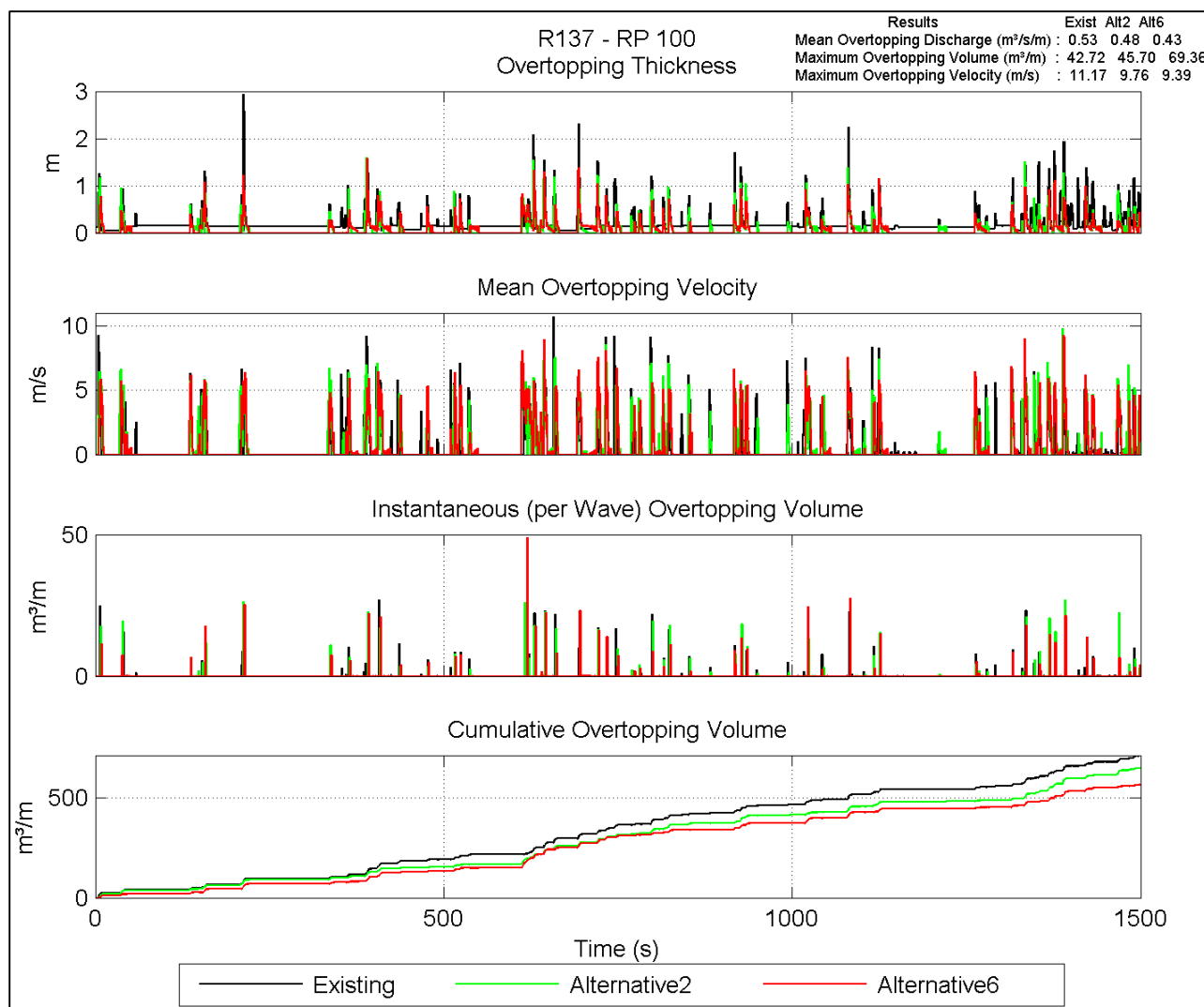


**Figure 3-24. Overtopping results - R-137 – 100-year return period for existing conditions (black), Alternative 2 (green), Alternative 6 (red).**

The mean overtopping discharges for the existing and alternatives are listed in Table 3-1. The safety guide presented in the Coastal Engineering Manual (USACE, 2006) identifies the mean overtopping discharge as an important parameter to consider for the traffic and structural safety criteria during the storm events (Figure 2-1). The safety criteria are specific at the point of overtopping (i.e. the dune crest and seawall) and do not indicate the safety criteria further landward.

**Table 3-1. Mean overtopping discharge summary for all cases.**

Profile	Condition	Return Period (years)	Mean Overtopping Discharge (m <sup>3</sup> /s/m)	Reduction in Overtopping
T-131	Existing Conditions	15	0.03	-
		25	0.08	
		50	0.31	
		100	0.77	
	Alternative 2/6	15	0.01	67 %
		25	0.02	75 %
		50	0.13	58 %
		100	0.24	69%
R-137	Existing Conditions	15	0.04	-
		25	0.09	
		50	0.25	
		100	0.53	
	Alternative 2	15	0.03	25 %
		25	0.09	0 %
		50	0.23	8 %
		100	0.48	9 %
	Alternative 6	15	<0.01	>75 %
		25	0.07	22 %
		50	0.21	16 %
		100	0.43	19 %

- Safety of Traffic – Once the mean overtopping discharge exceeds 0.00005 m<sup>3</sup>/s/m the criteria become “unsafe” for vehicles and “dangerous” for pedestrians. The IH2VOF model quantifies overtopping discharge to an accuracy of 0.01 m<sup>3</sup>/s/m. Thus, based on the overtopping simulated by the model, the vehicle safety criteria is expected to be “unsafe at any speed” and the pedestrian safety criteria is expected to be “very dangerous.”
- Structural Safety
  - A seawall exists at R-137. For the existing conditions, the top 3-4 feet of the seawall is exposed. In this circumstance, the structural safety of the seawall is most closely characterized by the “embankment seawalls”

category. During the 15-year return period storm, the overtopping discharge was estimated at  $0.04 \text{ m}^3/\text{s}/\text{m}$ , which would result in “damage if back slope is not protected.” During the 25, 50 and 100 return period storms, the overtopping discharge increases and would result in “damage even if fully protected.”

- The seawall at R-137 is buried for the alternatives resulting in a dune similar to the situation at T-131. In these circumstances at T-131 and R-137, the structural safety of the dune is most closely characterized by the “grass sea-dikes” category. According to USACE the “start of damage” is expected once the overtopping discharge exceeds  $0.001 \text{ m}^3/\text{s}/\text{m}$ . “Damage” is expected once an overtopping discharge of  $0.01 \text{ m}^3/\text{s}/\text{m}$  is exceeded. Based on the model results, the overtopping discharge exceeded  $0.01 \text{ m}^3/\text{s}/\text{m}$  indicating “damage” for all the return period storms under the existing conditions and the alternatives. However, there was an exception during the 15-year storm event for the alternatives. At T-131 for Alternative 2/6, the discharge was at the threshold between the “start of damage” and “damage.” At R-137 for Alternative 6, the discharge was less than  $0.01 \text{ m}^3/\text{s}/\text{m}$  within the range of “start of damage.”

#### 4.0 WAVE FORCES ON SEAWALL

Under existing conditions, the upland seawalls are exposed to wave attack. At R-137, the top 2-3 feet of the seawall is exposed with the existing conditions. The IH2VOF model was used to estimate the dynamic load at the seawall as shown in Figure 4-1. For existing conditions, all the return period storms simulated impacted the seawall. The maximum horizontal force for a return period waves of 15, 25, 50 and 100 years were 41.8, 53.3, 69.1 and 131.0 kN/m, respectively. The maximum horizontal momentum calculated by IH2VOF for existing conditions with return period waves of 15, 25, 50 and 100 years was 25.6, 37.2, 52.2 and 182.8 kN/m, respectively. Since the condition, age and structural integrity of the seawalls are unknown, it is not clear how these wave forces could impact

their ability to protect the upland areas. Adding sand fill in front of the seawalls may provide additional protection by buffering the wave attack.

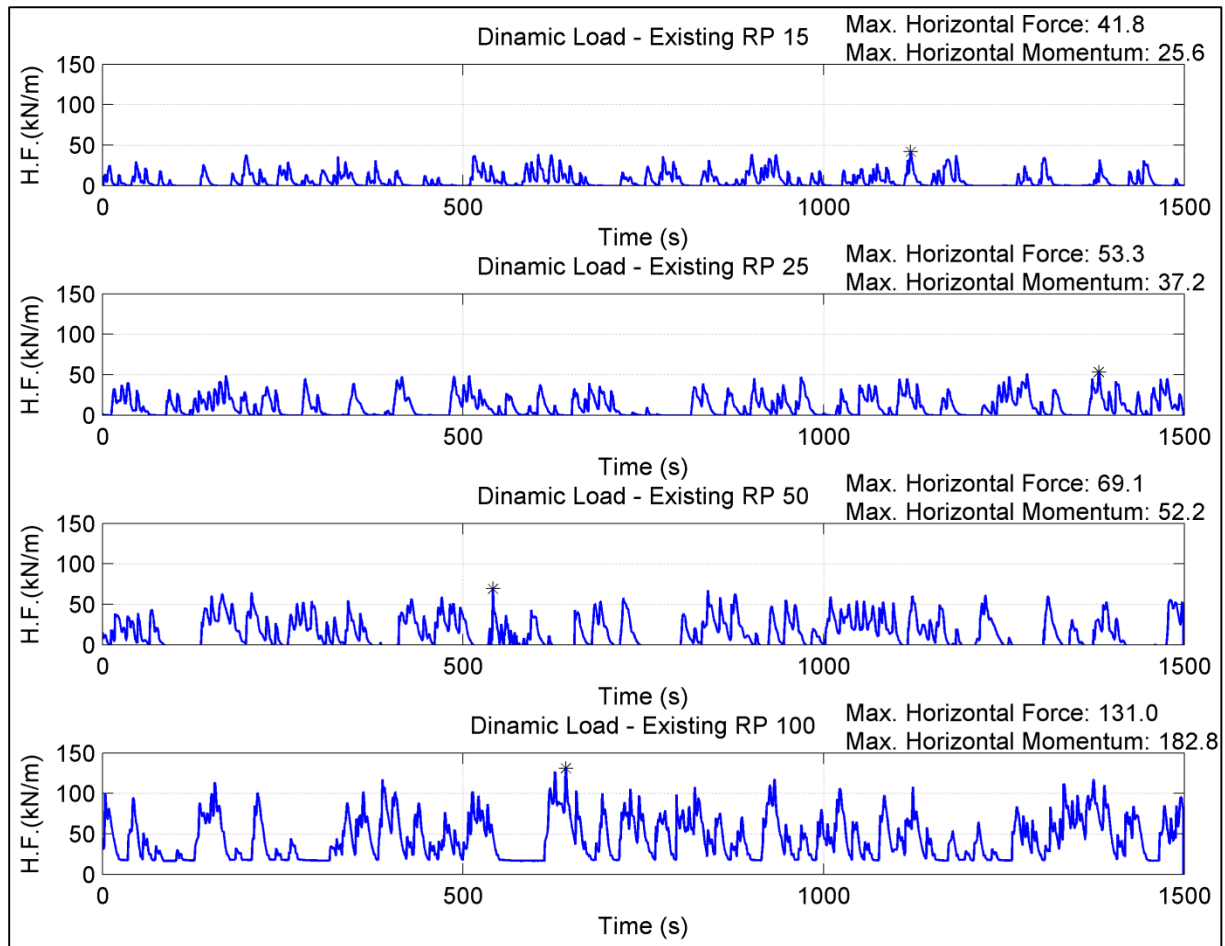


Figure 4-1. Dynamic load at seawall: top to bottom: Existing condition RP15, Existing condition RP25, Existing condition RP50, Existing condition RP100.

## 5.0 SUMMARY

The IH2VOF model was used to assess the potential overtopping during extreme conditions including the 15, 25, 50 and 100 years return period waves and water levels. Two profiles were analyzed, one without a seawall (T-131) and one with a seawall (R-137). The wave data and storm profiles were obtained from previous SBEACH modeling. The water level was considered constant during the simulation period (25 minutes). To analyze comparatively, four wave cases were simulated on each profile for two alternatives (Alternatives 2 and 6).

Seven probes were placed within the model across the beach profiles to analyze the evolution of wave propagation toward the coast. The probes showed a reduction in wave height as the waves propagated through shallower water depths and the transfer of wave energy from higher to lower frequencies due to wave breaking. The transfer of energy can eventually generate infragravity waves, which depending on a variety of factors including profile shape and elevation, can be more important than wave height on causing overtopping (Suzuki et al., 2012). As the waves approach the beach, the presence of the beach fill from Alternatives 2 and 6 reduced wave height, the likelihood of the waves reaching the dune crest, and the frequency of overtopping. It was also observed that as the waves and water levels increase, the overtopping thickness increases.

- 15-Year Return Period Storm: At T-131, the Alternatives 2/6 resulted in a 67% reduction in the mean overtopping discharge as compared to the existing conditions. At R-137, the volume of water overtopping the seawall was reduced by 25% for Alternative 2 and 88% for Alternative 6 as compared to the existing conditions.
- 25-Year Return Period Storm: At T-131, the overtopping discharge for Alternatives 2/6 is reduced by 75% as compared to the existing conditions. At R-137, overtopping discharge is similar for existing conditions and Alternative 2, while a 22% reduction was simulated for Alternative 6.

- 50-Year Return Period Storm: At T-131, the overtopping discharge for Alternatives 2/6 is reduced by 58% as compared to the existing conditions. At R-137, the reduction is observed, but at a smaller magnitude. For Alternatives 2 and 6 the mean overtopping discharges are reduced by 8% and 16% as compared to the existing conditions.
- 100-Year Return Period Storm: At T-131, the overtopping discharge for Alternatives 2/6 is reduced by 69% as compared to the existing conditions. At R-137, the reduction is observed, but at a smaller magnitude. For Alternatives 2 and 6 the mean overtopping discharges are reduced by 9% and 19% as compared to the existing conditions.

The top 1-3 feet of the seawall is exposed for the existing conditions and buried for the alternatives. For the exposed portion under the existing conditions, the results showed that the maximum horizontal forces at the seawall vary from 41.8, 53.3, 69.1 and 131.0 kN/m for 15, 25, 50 and 100 year return period waves, respectively. The maximum horizontal momentum for existing conditions with return period waves of 15, 25, 50 and 100 years was 25.6, 37.2, 52.2 and 182.8 kN/m, respectively. The wave forces and momentums to which the seawall is exposed increases with higher return period waves. Sand fill placed in front of the seawalls may reduce this effect.

The overtopping discharge was used to categorize the anticipated safety during the storm events. Regardless of the return period storm event, the overtopping is expected to be “unsafe at any speed” for vehicle safety and “very dangerous” pedestrian safety. At R-137 when the seawall is exposed under the existing conditions, “damage if back slope is not protected” should be expected for the 15-year return period storm event, and “damage even if fully protected” should be expected for the 25-, 50- and 100-year events. At T-131 and at R-137 (for the alternatives), the dune is expected to incur “damage” except during the 15-year return period storm event for Alternative 6. During this scenario, the additional protection provided by the increased fill volume would reduce the expectation to “start of damage.”

## 6.0 CONCLUSIONS

While considering the findings of this study, it is important to emphasize that the simulated conditions represent extreme storm events, but there is considerable variability among events that may be encountered. Based on the modeling, the following conclusions were made:

- The existing beach conditions are susceptible to wave overtopping during 15-, 25-, 50- and 100-year return period storms. Overtopping increases as wave and water level conditions increase. This is attributed to the reduction in dry beach width and the dune crest (or seawall) height above the waves and water level.
- For the return period storms, the alternatives provide a reduction in overtopping and consequently an increase in storm protection as compared to the existing conditions.
  - At T-131, the overtopping during the 15 year storm was reduced up to 67% for the alternatives as compared to the existing conditions. Similarly, the overtopping during 25-, 50- and 100-year storms were decreased up to 75%, 58% and 69%, respectively.
  - At R-137, the larger fill volume associated with Alternative 6 provided greater storm protection by reducing overtopping as compared to Alternative 2. The incremental benefit of Alternative 6 above the protection was 75% less overtopping for the 15 year return period storm, 22% less for the 25-year storm, 16% less for the 50-year storm, and 19% less for the 100 year storm as compared to the existing conditions. Alternative 2 provided 25% less overtopping for the 15-year storm, no improvement for the 25-year storm, 8% for the 50-year storm, and 9% for the 100-year storm.
- Given the existing conditions, seawalls are subject to wave attack during storm events. The wave forces that the seawalls are exposed to increase with the intensity of the storm events. The exposure of seawalls to waves can cause

damage thereby reducing the designed level of protection and/or increasing the frequency and need for structural repairs in order to maintain their integrity. Sand fill placed in front of the seawalls may offer additional protection.

- According to the USACE safety criteria, the mean overtopping discharge during the storm events is expected to cause some level of damage to the dune (or seawall) and create unsafe, dangerous situations for vehicles and pedestrians at the point of overtopping. Overtopping was not eliminated by having the alternatives in place. However, the alternatives did reduce overtopping, which would in turn reduce damage and unsafe, dangerous situations during storm events.

The results of this numerical modeling study should be used in conjunction with other coastal engineering assessments and prudent engineering judgment.

## 7.0 LITERATURE CITED

CB&I Coastal Planning & Engineering, Inc. 2014. Southern Palm Beach Island Comprehensive Shoreline Stabilization Project Environmental Impact Statement (EIS) SBEACH Analysis Report. Prepared for U.S. Army Corps of Engineers (USACE) 131 p.

EurOtop Manual. 2007. Overtopping Manual; Wave Overtopping of Sea Defences and Related Structures – Assessment Manual. UK: N.W.H. Allsop, T. Pullen, T. Bruce. NL: J.W. van der Meer. DE: H. Schüttrumpf, A. Kortenhaus. [www.overtopping-manual.com](http://www.overtopping-manual.com).

Hirt, C.W. and B.D. Nichols. 1981. Volume of Fluid (VOF) method for dynamics of the Free boundaries. *Journal of Computation Physic* 39: 201-225.

Hsu, T.-J., T. Sakakiyama, and P.L.-F. Liu. 2002. A Numerical Model for Wave Motions and Turbulence flows in Front of a Composite Breakwater. *Coastal Engineerint*, 46: 25-50.

Lykke Andersen, T. 2006. Hydraulic Response of Rubble Mound Breakwaters. Scale Effects – Berm Breakwaters, Ph.D. Thesis, Department of Civil Engineering, Aalborg University, Denmark.

Peng Z. and Q.-P. Zou. 2011. Spatial distribution of wave overtopping water behind coastal structures. *Coastal Engineering* 58: 489–498.

Schüttrumpf, H. and H. Oumeraci. 2005. Layer Thickness and Velocities of Overtopping at Seadikes. *Journal of Coastal Engineering* 52: 473-495.

Suzuki, T., T. Verwaest, W. Veale, K. Trouw, and M. Zijlema. 2012. A Numerical Study on the Effect of the Beach Nourishment on Wave Overtopping in Shallow Foreshores. *Coastal Engineering* 2012. 12 pp.

U.S. Army Corps of Engineers, 2006. Coastal Engineering Manual, Engineer Manual 1110-2-1100, U.S. Army Corps of Engineers, Washington, D.C. (in 6 volumes).

Van der Meer, J.W., R. Schrijver, B. Hardeman, A. van Hoven, H. Verheij and G.J. Steendam. 2009. Guidance on erosion resistance of inner slopes of dikes from three years of testing with the Wave Overtopping Simulator. Proc. ICE, Coasts, Marine Structures and Breakwaters 2009, Edinburgh, UK.